Cycle-Free Twisted Face-Pairing 3-Manifolds

Christopher J. Gartland

Dissertation submitted to the Faculty of the
Virginia Polytechnic Institute and State University
in partial fulfillment of the requirements for the degree of

Master of Science
in
Mathematics

William J. Floyd, Chair
Peter E. Haskell
Peter A. Linnell

May 13, 2014
Blacksburg, Virginia

Keywords: 3-manifolds, plumbing graphs, Seifert fibered spaces, face-pairings

Cycle-Free Twisted Face-Pairing 3-Manifolds

Christopher J. Gartland

(ABSTRACT)

In 2-dimensional topology, quotients of polygons by edge-pairings provide a rich source of examples of closed, connected, orientable surfaces. In fact, they provide all such examples. The 3-dimensional analogue of an edge-pairing of a polygon is a face-pairing of a faceted 3-ball. Unfortunately, quotients of faceted 3-balls by face-pairings rarely provide us with examples of 3-manifolds due to singularities that arise at the vertices. However, any face-pairing of a faceted 3-ball may be slighted modified so that its quotient is a genuine manifold, i.e. free of singularities. The modified face-pairing is called a twisted face-pairing. It is natural to ask which closed, connected, orientable 3-manifolds may be obtained as quotients of twisted face-pairings. In this paper, we focus on a special class of face-pairings called cycle-free twisted face-pairings and give description of their quotient spaces in terms of integer weighted graphs. We use this description to prove that most spherical 3-manifolds can be obtained as quotients of cycle-free twisted face-pairings, but the Poincaré homology 3-sphere cannot.

Acknowledgments

I would like to thank Dr. Bill Floyd and Dr. Walter Parry for their guidance on my research and for their helpful comments on writing this thesis.

I also thank my family for the support they provided me throughout my education.

Contents

List of Figures

List of Tables

0.1 Introduction

It is a well-known theorem in 2-dimensional topology that every closed, connected surface is homeomorphic to a quotient of a polygon by an identification of edges in pairs. Having such a concrete model of a surface allows one to answer many topological questions about the surface. For example, this result is often employed in proving the classification theorem of closed, connected surfaces. Furthermore, a certain converse to this result is true; every quotient of a polygon by an identification of edges in pairs is a closed, connected surface.

In 3-dimensional topology, there is an analogous, but more complex result. Firstly, an appropriate 3-dimensional analogue of a polygon is required. The analogue is a 3-dimensional CW-complex with underlying space the closed 3-ball, having exactly one 3-cell. Such a CW-complex is called a faceted 3-ball. It is then a theorem that every closed, connected, orientable 3-manifold is homeomorphic to a quotient of a faceted 3-ball by an orientation-reversing identification of faces in pairs, where two faces are identified only if they have the same number of edges. Such an identification is called a face-pairing. The analogous converse to this theorem, however, is false; a quotient of a faceted 3-ball by a face-pairing need not be a 3-manifold. In fact, in a certain sense, a quotient of a random faceted 3-ball by a random face-pairing will be a 3-manifold almost never, see Proposition 2.8 from Dunfield and Thurston [5], for example. The issue here is that the link of a vertex in the quotient may be a closed surface other than the 2-sphere, and such a vertex will be a singularity. In dimension 2, this issue cannot arise since the link of any vertex will be a closed, connected 1-manifold, and the only such manifold is the 1-sphere.

In [1] and [2], Cannon, Floyd, and Parry introduce a faceted 3-ball face-pairing method, called twisted face-pairing, for which the quotient is always a closed, connected, orientable 3-manifold. The method takes as input an arbitrary faceted 3-ball and face-pairing, called the model face-pairing, creates a new faceted 3-ball by subdividing edges in a carefully chosen way, and creates a face-pairing of the new faceted 3-ball based on the original face-pairing. The quotient of the new faceted 3-ball by the new face-pairing is called the twisted face-pairing 3-manifold based on the model face-pairing. In [4], they explored the question of which 3-manifolds are homeomorphic to twisted face-pairing manifolds. In Theorem 8.1 from [4], they were able to prove that 'most' Seifert fibered spaces are twisted face-pairing manifolds. Seifert fibered spaces have represented an important class of manifolds in 3-dimensional topology; for example, they account for all manifolds in six of the eight Thurston geometries, including those manifolds admitting spherical geometry, the spherical space forms. Theorem 8.1 from [4] proves that all but finitely many spherical space forms are twisted face-pairing manifolds, but it is not known whether or not the remaining spherical space forms are twisted face-pairing manifolds.

In this paper, we will focus on a certain class of twisted face-pairing 3-manifolds, a subclass of the twisted reflection face-pairing manifolds introduced in [4], called cycle-free twisted face-pairing manifolds. This class of manifolds contains many of the examples illustrated in [4], with the added benefit that the face-pairing description is particularly simple. Furthermore, we obtain necessary and sufficient conditions for a Seifert fibered space over S^2 (other than $S^2 \times S^1$) to belong to this class. Twisted face-pairing manifolds, Seifert fibers spaces, and spherical space forms are introduced in Chapter 1. To obtain the necessary and sufficient conditions, we draw from theorems in [4] giving Dehn surgery descriptions for twisted face-pairing manifolds, and theorems in [10], [7], and [8] about graph manifolds and the plumbing calculus and their relationships to Dehn surgery. We also introduce a new weighted graph structure called an EFe-labeling, and prove that the admittance of an EFe-labeling is a semi-invariant of the weighted graph under the plumbing calculus. This EFe-labeling structure is the topic of Chapter 2. Chapter 3 discusses manifolds plumbed from weighted graphs admitting an EFe-labeling, and their relationships to Seifert fibered spaces over S^2. Chapter 4 introduces the cycle-free twisted face-pairing manifolds, and Chapter 5 finally ties the results together into the main result of this paper, Theorem 5.1.5, which states the necessary and sufficient conditions for a Seifert fibered space over S^2 (other than $S^2 \times S^1$) to be homeomorphic to a cycle-free twisted face-pairing manifold in terms of the normalized Seifert invariants. Theorem 5.1.5 should be compared to Theorem 8.1 from [4] with respect to their implications on Seifert fibered spaces M over S^2 with normalized invariants $\{Oog\big|b; (\alpha_1, \beta_1), \ldots (\alpha_n, \beta_n)\}$ satisfying $n \geq 3$. The latter theorem implies M is a twisted face-pairing manifold if $b \geq 0$. The former theorem implies M is also a *cycle-free* twisted face-pairing manifolds if $b \geq 0$, and, conversely, M is *not* a cycle-free twisted face-pairing manifold if $b < 0$. Chapter 5 also includes an application of Theorem 5.1.5 to the spherical 3-manifolds.

Chapter 1

Preliminaries

1.1 Twisted Face-Pairing Manifolds

The theory of twisted face-pairing manifold was developed by Cannon, Floyd, and Parry in a series of papers starting with [1] in 2000, and including [2], [3], and [4] through 2002. A reading of those papers in that order would provide a thorough treatment of the topic. We will introduce the basic construction here and state the fundamental theorem from [1].

We follow Section 2 from [2] in this discussion. A *faceted 3-ball* will be a regular, oriented CW-complex P with underlying space $B^3 = \{(x, y, z) \in \mathbb{R}^3 : x^2 + y^2 + z^2 \leq 1\}$ such that P has exactly one open 3-cell, namely the interior, $P - \partial(P)$. Then the data of a faceted 3-ball is completely determined by a regular CW-complex structure on $S^2 = \partial(B^3)$. A *face-pairing* ϵ on a faceted 3-ball P consists of a partition of the closed faces into pairs, $\{\{F_i, F_i^{-1}\}\}_i$ (with the notational convention that $(F_i^{-1})^{-1} = F_i$), and an orientation-reversing cellular homeomorphism $\epsilon_i : F_i \to F_i^{-1}$ for each pair. We set $\epsilon = \{\epsilon_i, \epsilon_i^{-1}\}_i$. ϵ also must satisfy a compatibility condition which we will describe shortly. If E is any edge of F_{i_1}, then $\epsilon_{i_1}(E)$ is an edge of $F_{i_1}^{-1}$. Then $\epsilon_{i_1}(E)$ is contained in exactly one other face of $\partial(P)$ other than $F_{i_1}^{-1}$, say F_{i_2}. Then $\epsilon_{i_2}(\epsilon_{i_1}(E)) = (\epsilon_{i_2} \circ \epsilon_{i_1})(E)$ is an edge of $F_{i_2}^{-1}$. Continuing in this way, we obtain a sequence of maps ϵ_{i_1}, $\epsilon_{i_2} \circ \epsilon_{i_1}$, $\epsilon_{i_3} \circ \epsilon_{i_2} \circ \epsilon_{i_1}$, ... that send E to different edges of $\partial(P)$. Eventually, we must have $(\epsilon_{i_k} \circ \ldots \epsilon_{i_1})(E) = E$ for some k. The set $\{(\epsilon_{i_j} \circ \ldots \epsilon_{i_1})(E)\}_{j=1}^{k}$ is called *an edge cycle* of ϵ, and also *the edge cycle* of E, notated $[E]$. We note that the collection of edge cycles partitions the full set of edges of P. The compatibility condition required for ϵ is that $(\epsilon_{i_k} \circ \ldots \epsilon_{i_1})\big|_E$ is the identity map on E, for each edge E of $\partial(P)$. We note that a face-pairing on a faceted 3-ball P exists if and only if the closed faces of P have a partition into pairs $\{F_i, F_i^{-1}\}_i$ where F_i and F_i^{-1} have the same number of edges.

We now pause to illustrate these constructions with an example. In Figure 1.1, we have

a diagram of a regular CW-complex with underlying space S^2, and we have labeled the 4 edges a, b, c, and d and the 4 faces F_1, F_2, F_1^{-1}, and F_2^{-1}. The diagram in the figure is not actually of S^2, but of the stereographic projection of S^2 minus the centroid of F_1^{-1} onto the plane. Thus, F_1^{-1} appears as an unbounded component.

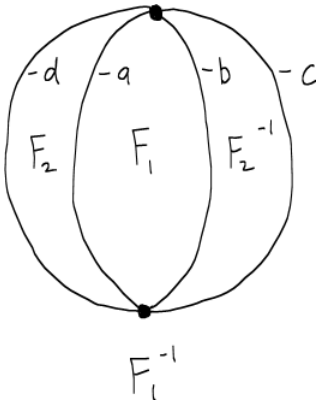

Figure 1.1: Diagram of stereographic projection of cell structure on S^2 onto the plane. This cell structure determines a faceted 3-ball P such that $\partial(P)$ is shown in the diagram.

We let P be the faceted 3-ball whose boundary cell structure is that shown in Figure 1.1. Thus, P is a solid globe with 4 longitude lines connecting vertices located on the north and south poles. We let ϵ_1 be the restriction of the antipodal map on S^2 to F_1 and ϵ_2 the restriction of the antipodal map to F_2. Then $\{\{F_1, F_1^{-1}\}, \{F_2, F_2^{-1}\}\}$ is a partition of the faces of $\partial(P)$ into pairs, and each $\epsilon_i : F_i \to F_i^{-1}$ is an orientation-reversing cellular homeomorphism, so $\epsilon = \{\epsilon_1, \epsilon_1^{-1}, \epsilon_2, \epsilon_2^{-1}\}$ is a face-pairing on P. The action of ϵ_1 and ϵ_2 on the edges of F_1 and F_2 is shown in Table 1.1.

Table 1.1: Actions of orientation-reversing cellular homeomorphisms ϵ_1 and ϵ_2 on edges of F_1 and F_2.

E	a	b
$\epsilon_1(E)$	c	d

E	d	a
$\epsilon_2(E)$	b	c

By starting at a and b in the table and following their images, we have the diagrams of mappings

$$a \xrightarrow{\epsilon_1} c \xrightarrow{\epsilon_2^{-1}} a$$

$$b \xrightarrow{\epsilon_1} d \xrightarrow{\epsilon_2^{-1}} b$$

Every edge is included in one of these diagrams, so the edge cycles of ϵ are $\{a, c\}$ and $\{b, d\}$.

Now, given an arbitrary faceted 3-ball P and face-pairing ϵ, let $\sim$ be the equivalence relation on P generated by $\{(p, \epsilon_i(p)) \in P \times P : p \in F_i, F_i \text{ is closed face of } P\}$. Then we define P/ϵ to be the quotient space $P/\sim$, so P/ϵ is obtained from P by gluing faces together along ϵ. P/ϵ will be compact and connected since P is, and P/ϵ inherits an orientation from P since the maps constituting ϵ are orientation-reversing. The compatibility condition on ϵ also ensures that P/ϵ inherits a cell structure from P, where the 3-cell of P/ϵ is identified with the 3-cell of P, a face of P/ϵ is identified with a pair of faces of P, an edge of P/ϵ is identified with an edge cycle of P, and a vertex of P/ϵ is identified with a set of vertices of P. Furthermore, if p is a point of P that is not a vertex, the image of p in P/ϵ will have a Euclidean neighborhood. This implies that P/ϵ minus its set of vertices is a 3-manifold, without boundary. Of course, this space will no longer be compact. Furthermore, it is often the case that a vertex of P/ϵ will not have a Euclidean neighborhood, so P/ϵ is *not* a manifold. In fact, in a certain sense, if (P, ϵ) is chosen at random, P/ϵ will be a manifold with probability 0. This is formalized in Proposition 2.8 from [5], which deals with random gluings of tetrahedra.

Returning to our example (P, ϵ) with $\partial(P)$ as in Figure 1.1, we find that $P/\epsilon = B^3/(\text{antipodal map}) \approx \mathbb{R}P^3$. In this case, it happens that P/ϵ is a manifold.

Given an arbitrary faceted 3-ball P with face-pairing ϵ, we describe a modification that produces another faceted 3-ball Q with face-pairing δ. Let $\{[E]_i\}_i^k$ be the set of edge cycles of ϵ, ordered in some way, as defined in the previous paragraph. Let $mult = \{m_i\}_{i=1}^k \subseteq \mathbb{Z}_{>0}$ be a sequence of positive integers. We call $mult$ a *multiplier function* for ϵ. Then we define $Q = Q(\epsilon, mult)$ to be the faceted 3-ball obtained from P by subdividing each edge E of E into $|[E]_i| \cdot m_i$ edges, where $|[E]_i|$ is the number of edges in the edge cycle of E, and m_i is the corresponding positive integer from $mult$. We require that the subdivision respects ϵ, meaning that each ϵ_i is still a cellular homeomorphism when viewed as a map on the new subdivided face (so the newly added vertices in the subdivision map to newly added vertices under ϵ_i). For each closed face F_i of Q, let τ_i be an orientation-preserving cellular automorphism of F_i that sends each vertex to its succeeding vertex under the cyclic order induced by the orientation. Let $\delta_i = \epsilon_i \circ \tau_i$, and $\delta = \{\delta_i\}_i$. Then δ is a face-pairing on Q. We define $M = M(\epsilon, mult) = Q/\delta$ to be the *twisted face-pairing manifold* modeled on the face-pairing (P, ϵ). Note that we chose the map τ_i arbitrarily in the construction. But the properties we required that τ possess uniquely determines its action on vertices, and the homeomorphism class of the quotient space Q/δ only depends on this data (this is mentioned on page 3 of [1]). As the naming suggests, we have the following Main Theorem from Section 2 of [1].

Theorem 1.1.1. For any faceted 3-ball P with face-pairing ϵ and multiplier function $mult$ corresponding to the edge cycles of ϵ, the associated twisted face-pairing manifold $M(\epsilon, mult)$

is a closed, connected, oriented 3-manifold.

We again return to our example (P, ϵ) from Figure 1.1. Our ordered set of edge cycles in this case is $(\{a, c\}, \{b, d\})$, so $mult = (1, 2)$ is an allowable multiplier function, since the cardinalities match. So we then need to subdivide a and c into $|\{a, c\}| \cdot 1 = 2$ edges and b and d into $|\{b, d\}| \cdot 2 = 4$ edges. The stereographic projection of $\partial(Q)$ is shown in Figure 1.2. The newly added vertices are shown in pink. The subdivided edges have been labeled.

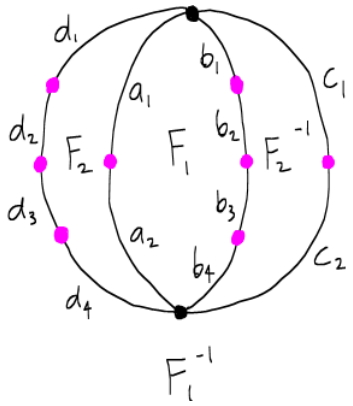

Figure 1.2: Diagram of stereographic projection of $\partial(Q)$ onto the plane. $\partial(Q)$ is obtained from $\partial(P)$ by subdividing edges. The newly added vertices are shown in pink. The subdivided edges have been labeled.

We choose an orientation of P that induces a clockwise orientation on the faces. Then the maps τ_1 and τ_2 are orientation-preserving cellular automorphisms of F_1 and F_2 whose action on edges is shown in Table 1.2.

Table 1.2: Action of orientation-preserving cellular automorphisms τ_1 and τ_2 on edges of F_1 and F_2.

E	a_1	b_1	b_2	b_3	b_4	a_2
$\tau_1(E)$	b_1	b_2	b_3	b_4	a_2	a_1

E	d_1	a_1	a_2	d_4	d_3	d_2
$\tau_2(E)$	a_1	a_2	d_4	d_3	d_2	a_1

Since $\delta_i = \epsilon_i \circ \tau_i$, we combine the information from Tables 1.1 and 1.2 to obtain Table 1.3.

Table 1.3: Action of orientation-reversing cellular homeomorphisms δ_1 and δ_2 on edges of F_1 and F_2.

E	a_1	b_1	b_2	b_3	b_4	a_2
$\delta_1(E)$	d_4	d_3	d_2	d_1	c_1	c_2

E	d_1	a_1	a_2	d_4	d_3	d_2
$\delta_2(E)$	c_2	c_1	b_1	b_2	b_3	b_4

By starting at a_1 and d_1 in the table and following their images, we have the diagrams of mappings

$$a_1 \xrightarrow{\delta_1} d_4 \xrightarrow{\delta_2} b_2 \xrightarrow{\delta_1} d_2 \xrightarrow{\delta_2} b_4 \xrightarrow{\delta_1} c_1 \xrightarrow{\delta_2^{-1}} a_1$$

$$d_1 \xrightarrow{\delta_2} c_2 \xrightarrow{\delta_1^{-1}} a_2 \xrightarrow{\delta_2} b_1 \xrightarrow{\delta_1} d_3 \xrightarrow{\delta_2} b_3 \xrightarrow{\delta_1} d_1$$

Every edge is included in one of these diagrams, so the edge cycles of δ are $\{a_1, d_4, b_2, d_2, b_4, c_1\}$ and $\{d_1, c_2, a_2, b_1, d_3, b_3\}$. We let $\delta = \{\delta_1, \delta_1^{-1}, \delta_2, \delta_2^{-1}\}$, so then our twisted face-pairing manifold is the closed, connected, oriented 3-manifold $M = M(\epsilon, mult) = Q/\delta$. Since we have 2 face-pairs and 2 edge cycles of δ, it follows that the quotient complex Q/δ has 2 faces and 2 edges. It is also immediate that Q/δ has 1 3-cell, and it can also be seen that it has 1 vertex. Then the Euler characteristic of M is $1 - 2 + 2 - 1 = 0$. This is a property of closed, orientable 3-manifolds, and, in fact, the proof in [1] of our Theorem 1.1.1 relies on that fact that twisted face-pairing manifolds always have Euler characteristic 0. More can be said about M; it is a well-known consequence of the Seifert-van Kampen theorem that the fundamental group of M has a presentation with generators being δ_1 and δ_2 and relators being the words spelled out by the sequence of mappings giving the edge cycles above. In other words,

$$\pi_1(M) \cong \left\langle \delta_1, \delta_2 \middle| \delta_1\delta_2\delta_1\delta_2\delta_1\delta_2^{-1}, \delta_2\delta_1^{-1}\delta_2\delta_1\delta_2\delta_1 \right\rangle$$

This group turns out to be finite of order 24, which can be calculated by a coset enumeration algorithm, so M is a spherical space form by the elliptization theorem. A Smith normal form calculation also yields $H_1(M) \cong \pi_1(M)^{\text{ab}} \cong \mathbb{Z}_8$.

A special class of twisted face-pairing manifolds are the *twisted reflection face-pairing manifolds*, introduced in Section 3 of [4]. These are manifolds $M(\epsilon, mult)$ arising from a reflection face-pairing across the xy-plane. More precisely, every $\epsilon_i \in \epsilon = \{\epsilon_i\}_i$ is the restriction of the reflection map $(x, y, z) \mapsto (x, y, -z)$ to a face of P, where P is some faceted 3-ball. If P is a faceted 3-ball with reflection face-pairing ϵ, then P/ϵ is always homeomorphic to S^3. This is perhaps the simplest model face-pairing possible.

Figure 1.3 shows a diagram of a regular CW-complex with underlying space S^2. We have labeled the 9 edges a, b, c, d, e, f, g, h, and i, and the 8 faces F_1, F_2, F_3, F_4, F_1^{-1}, F_2^{-1}, F_3^{-1}, and F_4^{-1}. The diagram in the figure is not actually of S^2, but of the stereographic

projection of S^2 minus the centroid of F_1^{-1} (which we think of as the south pole) onto the plane. Thus, F_1^{-1} appears as an unbounded component. The intersection of S^2 with the xy-plane is shown in blue.

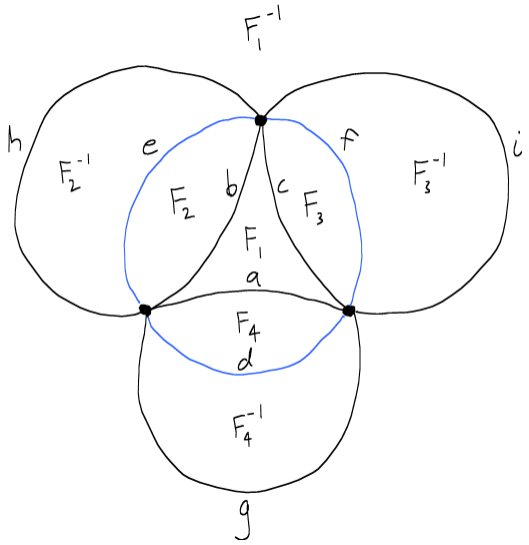

Figure 1.3: Diagram of stereographic projection of a cell structure on S^2 onto the plane. The blue circle represents the intersection of S^2 with the xy-plane. This cell structure determines a faceted 3-ball P such that $\partial(P)$ is shown in the diagram.

We let P be the faceted 3-ball whose boundary cell structure is that shown in Figure 1.3. We think of the region inside the blue circle as the northern hemisphere and the region outside the blue circle as the southern hemisphere. We let ϵ_i be the restriction to F_i of the reflection through the xy-plane, and we let and $\epsilon = \{\epsilon_i, \epsilon_i^{-1}\}_{i=1}^4$. Then ϵ is a reflection face-pairing. The set of edge cycles of ϵ is $(\{a, g\}, \{b, h\}, \{c, i\}, \{e\}, \{f\}, \{g\})$, and we order them in that order. Now, we let $mult = (1, 1, 1, 1, 2, 1)$. Then the number of edge subdivisions we needs to perform are 2, 2, 2, 1, 2, and 1, respectively. The resulting complex $\partial(Q)$ is shown in Figure 1.4. The newly added vertices are shown in pink. The subdivided edges have been labeled.

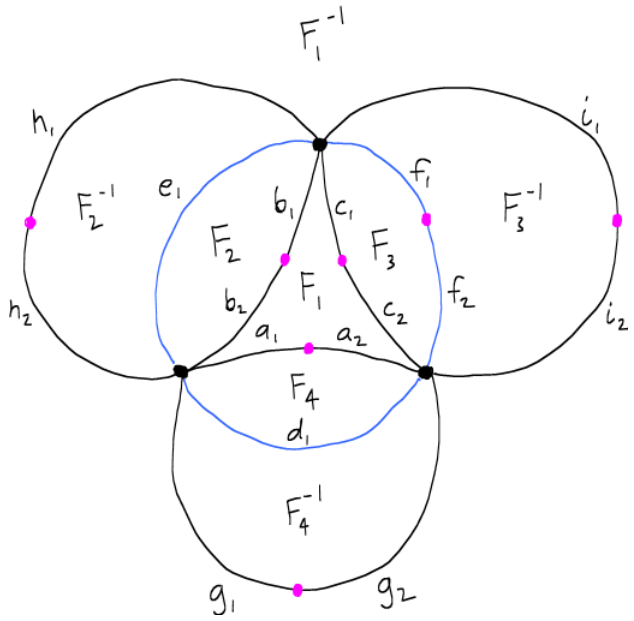

Figure 1.4: Diagram of stereographic projection of $\partial(Q)$ onto the plane. $\partial(Q)$ is obtained from $\partial(P)$ by subdividing edges. The newly added vertices are shown in pink. The subdivided edges have been labeled.

We orient P (and thus Q) so that τ_i is a clockwise twist for each i, and we let $\delta_i = \epsilon_i \circ \tau_i$. Table 1.4 shows that action of each δ_i on the edges of F_i.

Table 1.4: Action of orientation-reversing cellular homeomorphism δ_i on edges of F_i.

E	a_1	b_2	b_1	c_1	c_2	a_2
$\delta_1(E)$	h_2	h_1	i_1	i_2	g_2	g_1

E	e_1	b_1	b_2
$\delta_2(E)$	h_1	h_2	e_1

E	c_1	f_1	f_2	c_2
$\delta_3(E)$	f_1	f_2	i_2	i_1

E	d_1	a_1	a_2
$\delta_4(E)$	g_1	g_2	d_1

As before, we can start with an edge and use the table to follow its images under δ. This gives us the diagrams

$$a_1 \xrightarrow{\delta_1} h_2 \xrightarrow{\delta_2^{-1}} b_1 \xrightarrow{\delta_1} i_1 \xrightarrow{\delta_3^{-1}} c_2 \xrightarrow{\delta_1} g_2 \xrightarrow{\delta_4^{-1}} a_1$$

$$e_1 \xrightarrow{\delta_2} h_1 \xrightarrow{\delta_1^{-1}} b_2 \xrightarrow{\delta_2} e_1$$

$$c_1 \xrightarrow{\delta_3} f_1 \xrightarrow{\delta_3} f_2 \xrightarrow{\delta_3} i_2 \xrightarrow{\delta_1^{-1}} c_1$$

$$d_1 \overset{\delta_4}{\to} g_1 \overset{\delta_1^{-1}}{\to} a_2 \overset{\delta_4}{\to} d_1$$

Again, this leads to the following presentation for $\pi_1(M) = \pi_1(M(\epsilon, mult)) = \pi_1(Q/\delta)$:

$$\pi_1(M) \cong \left\langle \delta_1, \delta_2, \delta_3, \delta_4 \middle| \delta_1\delta_2^{-1}\delta_1\delta_3^{-1}\delta_1\delta_4^{-1}, \delta_2\delta_1^{-1}\delta_2, \delta_3\delta_3\delta_3\delta_1^{-1}, \delta_4\delta_1^{-1}\delta_4 \right\rangle$$

A coset enumeration calculation reveals $|\pi_1(M)| = 60$, so M is spherical, and a Smith normal form calculation yields $H_1(M) \cong \pi_1(M)^{\text{ab}} \cong \mathbb{Z}_4 \times \mathbb{Z}_5$.

A special subclass of the twisted reflection face-pairing manifolds are the *cycle-free twisted face-pairing manifolds*, which arise from model face-pairings where the faceted 3-ball has all its vertices on the equator. We formally introduce cycle-free twisted face-pairing manifolds in Definition 4.2.1. This class of manifolds is the focus of the paper, and we develop machinery in Chapters 2, 3, and 4 to understand its intersection with the class of Seifert fibered spaces and spherical space forms. Our main result is Theorem 5.1.5, where we obtain necessary and sufficient conditions for a Seifert fibered space over S^2 (other than $S^2 \times S^1$) to be a cycle-free twisted face-pairing manifold.

We note that our discussion of face-pairing in this chapter required faceted 3-balls to be regular CW-complexes. In the rest of this paper, we will actually use the definition of faceted 3-ball in Section 2 from [3]. A faceted 3-ball in this sense means a CW-complex (not necessarily regular) with underlying space the closed 3-ball, having exactly one open 3-cell, and such that the cell structure on the boundary does not consist of just one face and one vertex. A well-defined notion of face-pairing may be defined for this class of cell structures which generalizes our construction of this chapter, and the reader should consult Section 2 of [3] for the details.

1.2 Seifert Fibered Spaces

There is a special class of 3-manifolds called *Seifert fibered spaces* that have played a very important role in the history of 3-dimensional topology. Thurston's famous geometrization conjecture, now proved by Perelman, posits that every closed, orientable, prime 3-manifold admits a decomposition along certain embedded tori so that the interior of the complementary pieces admit finite volume geometric structures. A 3-manifold is said to *admit a geometric structure* if it is homeomorphic to the quotient of one of the eight Thurston model geometries by a free action of a discrete group of isometries. The eight model geometries are E^3, S^3, $\mathbb{H}^3$, $S^2 \times \mathbb{R}$, $\mathbb{H}^2 \times \mathbb{R}$, $\widetilde{\text{SL}}(2, \mathbb{R})$, Nil, and Solv. A closed 3-manifold admits a geometry based on E^3, S^3, $S^2 \times \mathbb{R}$, $\mathbb{H}^2 \times \mathbb{R}$, $\widetilde{\text{SL}}(2, \mathbb{R})$, or Nil if and only if it is a Seifert fibered space, so Seifert fibered spaces constitute six of the eight Thurston geometries. There is also a second decomposition of prime, closed, orientable 3-manifolds along embedded tori called the JSJ

decomposition. The compact pieces making up the decomposition are either Seifert fibered or atoroidal.

We now discuss the topological construction of closed, connected, oriented Seifert fibered spaces. Our discussion in this paragraph and notation throughout the paper follow that from Chapter 4 of [6]. A Seifert fibered space is completely determined by a set of invariants $\{Oog\big|b;(\alpha_1,\beta_1),\dots(\alpha_n,\beta_n)\}$ or $\{Onk\big|b;(\alpha_1,\beta_1),\dots(\alpha_n,\beta_n)\}$, where the symbols "$Oo$" and "$On$" are constants meaning orientable total space and orientable base space, and orientable total space and nonorientable base space, respectively, and g, k, b, n, α_i, and β_i are variables subject to $g\in\mathbb{Z}_{\geq 0}$, $k\in\mathbb{Z}_{>0}$, $b\in\mathbb{Z}$, $n\in\mathbb{Z}_{\geq 0}$, $\alpha_i\in\mathbb{Z}_{\geq 2}$, $\beta_i\in\mathbb{Z}$, and $(\alpha_i,\beta_i)=1$ for all i. We can also add the requirement that $0<\beta_i<\alpha_i$, in which case we call the invariants *normalized*. Every Seifert fibered space admits a set of normalized invariants. We now describe how to construct the topological space from a set of invariants. We start with a base space Σ, which is the closed, orientable surface of genus g if our invariants contain Oog, or the it is the closed, nonorientable surface with k cross-caps if our invariants contain Onk. We then form the oriented circle bundle $S^1\hookrightarrow M'\xrightarrow{\pi}\Sigma$ over Σ with Euler class $-b$. The Euler class can be seen as an obstruction to the existence of a section of π since π has a section if and only if its Euler class is 0. We then perform surgeries of type $\frac{\alpha_1}{\beta_1},\dots\frac{\alpha_n}{\beta_n}$ along n disjoint fibers of M' to obtain our Seifert fibered space M. M is said to be Seifert fibered over Σ with n exceptional fibers.

We further mention that if we change the set of invariants $\{O^{og}_{nk}\big|b;(\alpha_1,\beta_1),\dots(\alpha_i,\beta_i),\dots(\alpha_n,\beta_n)\}$ to $\{O^{og}_{nk}\big|b\mp 1;(\alpha_1,\beta_1),\dots(\alpha_i,\beta_i\pm\alpha_i),\dots(\alpha_n,\beta_n)\}$ for any $1\leq i\leq n$, the corresponding Seifert fibered spaces are orientation-preservingly homeomorphic. Every Seifert fibered space admits a set of normalized invariants, meaning $0<\beta_i<\alpha_i$ for all i, since an unnormalized set of invariants can be normalized by repeatedly applying this move. If M has invariants $\{O^{og}_{nk}\big|b;(\alpha_1,\beta_1),\dots(\alpha_n,\beta_n)\}$, then $-M$, the orientation reversal of M, has invariants $\{O^{og}_{nk}\big|-b;(\alpha_1,-\beta_1),\dots(\alpha_n,-\beta_n)\}$. It follows that if M has normalized invariants $\{O^{og}_{nk}\big|b;(\alpha_1,\beta_1),\dots(\alpha_n,\beta_n)\}$, then $-M$ has normalized invariants $\{O^{og}_{nk}\big|-b-n;(\alpha_1,\alpha_1-\beta_1),\dots(\alpha_n,\alpha_n-\beta_n)\}$.

Example:

Consider the normalized set of invariants $\{Oo1\big|0\}$. The base space is the closed surface of genus 1, which is the torus, T^2. The total space is the oriented circle bundle over T^2 with Euler class 0. Since the Euler class is 0, the bundle has a section, implying it is trivial, so our Seifert fibered space in this case is $T^3=S^1\times S^1\times S^1$.

Example:

If our normalized set of invariants is $\{Oo0\big|-1\}$, the base space is S^2, and the total space

is the oriented circle bundle over S^2 with Euler class 1. This bundle is the famous Hopf fibration, with total space S^3.

Example:

If our normalized set of invariants is $\{Oo0\big|-1;(2,1),(3,1),(5,1)\}$, the base space is S^2, and the total space is the oriented circle bundle over S^2 with Euler class 1 with surgeries of type 2, 3, and 5 performed. This Seifert fibered space is called the *Poincaré homology 3-sphere*. It is called a homology 3-sphere since it has the same homology groups as S^3. However, its fundamental group has order 120, so is not homeomorphic to S^3. Apart from S^3, it is the only homology 3-sphere with finite fundamental group.

1.3 Spherical Space Forms

We have already introduced what is meant by a 3-manifold admitting a geometric structure. A *spherical space form*, or *spherical 3-manifold* is a 3-manifold admitting a spherical geometry. Equivalently, M is a spherical space form if there exists a finite subgroup Γ of $\mathrm{Isom}(S^3) \cong \mathrm{O}(4)$ acting freely on M such that $M \approx S^3/\Gamma$. In this case, $\pi_1(M) \cong \Gamma$. Since Γ acts freely on S^3, $\Gamma \subseteq \mathrm{SO}(4)$, so Γ is orientation-preserving. Then S^3/Γ inherits an orientation from S^3. In many cases, it also happens that $S^3/\Gamma_1 \approx S^3/\Gamma_2$ if $\Gamma_1 \cong \Gamma_2$. So then the spherical space forms can nearly be classified by their fundamental groups, which in turn are identified with finite subgroups of $SO(4)$ that act freely on S^3. From page 112 of [9], each of these groups belongs to one of five disjoint families we discuss next.

Cyclic:

Γ is cyclic. In this case, S^3/Γ is called a *lens space*. The fundamental group of a lens spaces does not determine its homeomorphism type, or even its homotopy type. These are the only spherical space forms whose homeomorphism types are not determined by the fundamental group. Each oriented lens space is orientation-preservingly homeomorphic to infinitely many Seifert fibered spaces over S^2 with invariants of the form $\{Oo0\big|b;(\alpha_1,\beta_1),\dots(\alpha_n,\beta_n)\}$ with $0 \le n \le 2$. Conversely, all Seifert fibered spaces other than $S^2 \times S^1$ with normalized invariants of the form $\{Oo0\big|b;(\alpha_1,\beta_1),\dots(\alpha_n,\beta_n)\}$, $0 \le n \le 2$, are lens spaces.

Dihedral:

Γ is the product of a cyclic group and a central extension of a dihedral group. In this case, S^3/Γ is called a *prism manifold*. The fundamental group of a prism manifold determines its homeomorphism type. Each oriented prism manifold is orientation-preservingly homeomorphic to a unique Seifert fibered space over S^2 with normalized invariants of the form $\{Oo0\big|b;(2,1),(2,1),(\alpha_3,\beta_3)\}$. Conversely, all Seifert fibered spaces with normalized invari-

ants of the form $\{Oo0\big|b;(2,1),(2,1),(\alpha_3,\beta_3)\}$ are prism manifolds.

Tetrahedral:

Γ is the product of a cyclic group and a central extension of the tetrahedral group. The fundamental group of S^3/Γ determines its homeomorphism type. All oriented manifolds of this type are orientation-preservingly homeomorphic to a unique Seifert fibered space over S^2 with normalized invariants of the form $\{Oo0\big|b;(2,1),(3,\beta_2),(3,\beta_3)\}$. Conversely, all Seifert fibered spaces with normalized invariants of the form $\{Oo0\big|b;(2,1),(3,\beta_2),(3,\beta_3)\}$ fall into the tetrahedral family.

Octahedral:

Γ is the product of a cyclic group and the binary octahedral group, O^*. The fundamental group of S^3/Γ determines its homeomorphism type. All oriented manifolds of this type are orientation-preservingly homeomorphic to a unique Seifert fibered space over S^2 with normalized invariants of the form $\{Oo0\big|b;(2,1),(3,\beta_2),(4,\beta_3)\}$. Conversely, all Seifert fibered spaces with normalized invariants of the form $\{Oo0\big|b;(2,1),(3,\beta_2),(4,\beta_3)\}$ fall into the octahedral family.

Icosahedral:

Γ is the product of a cyclic group and the binary icosahedral group, I^*. The fundamental group of S^3/Γ determines its homeomorphism type. In the case $\Gamma = I^*$, S^3/Γ is the Poincaré homology 3-sphere. All oriented manifolds of this type are orientation-preservingly homeomorphic to a unique Seifert fibered space over S^2 with normalized invariants of the form $\{Oo0\big|b;(2,1),(3,\beta_2),(5,\beta_3)\}$. Conversely, all Seifert fibered spaces with normalized invariants of the form $\{Oo0\big|b;(2,1),(3,\beta_2),(5,\beta_3)\}$ fall into the icosahedral family. The Poincaré homology 3-sphere is homeomorphic to the Seifert fibered space with normalized invariants $\{Oo0\big|-1;(2,1),(3,1),(5,1)\}$.

So every oriented spherical manifold admits a representation as a Seifert fibered space over S^2, and, except for lens spaces, the corresponding normalized invariants are unique. This follows from the last paragraph of page 456 from Scott, [11]. Any non-lens space oriented spherical manifold has a normalized set of invariants of the form $\{Oo0\big|b;(2,1),(\alpha_2,\beta_2),(\alpha_3,\beta_3)\}$, so its orientation reversal has normalized invariants of the form
$\{Oo0\big|-b-3;(2,1),(\alpha_2,\alpha_2-\beta_2),(\alpha_3,\alpha_3-\beta_3)\}$, as discussed in the last section. It follows that if we ignore orientation, then every non-lens space has exactly two normalized sets of invariants, one of the form $\{Oo0\big|b;\dots\}$ and the other of the form $\{Oo0\big|-b-3;\dots\}$. Exactly one of $\{b,-b-3\}$ will be no less than -1, so we deduce the following classification theorem:

Theorem 1.3.1. Every non-lens space spherical space form M is (orientation-preservingly

or -reversingly) homeomorphic to exactly one Seifert fibered space over S^2 with normalized invariants $\{Oo0\big|b;(2,1),(\alpha_2,\beta_2),(\alpha_3,\beta_3)\}$ satisfying $b \geq -1$. If $\alpha_2 = 2$, then M is a prism manifold. If $\alpha_2 = \alpha_3 = 3$, then M belongs to the tetrahedral family. If $\alpha_2 = 3$ and $\alpha_3 = 4$, then M belongs to the octahedral family. If $\alpha_2 = 3$ and $\alpha_3 = 5$, then M belongs to the icosahedral family. Up to permutations of the indices, these all are the values that can be attained by α_i for M a spherical manifold.

Chapter 2

EFe-Labeled Graphs

We begin by developing the main tools we will use to study cycle-free twisted face-pairing manifolds: weighted graphs and EFe-labeled graphs. Weighting are defined in Definition 2.0.3, and EFe-labelings are defined in Definition 2.0.6.

Definition 2.0.2. In this paper, a **graph** will mean a finite, simple graph. In particular, this means there are only finitely many vertices and edges of the graph, the edges are undirected, each edge contains exactly two vertices, and given any two distinct vertices of the graph, there is at most one edge that contains both of them. The **valence** of a vertex is the total number of edges that contain the vertex. If v_1 and v_2 are vertices contained in an edge, we often say that v_1 and v_2 are "adjacent" or "connected by an edge". The former is especially used when one of the two vertices has valence 1 or 2. $\boldsymbol{V(\Gamma)}$ and $\boldsymbol{E(\Gamma)}$ will denote the set of vertices and the set of edges, respectively, of the graph Γ. As a convention, when drawing local diagrams of graphs, a picture of a vertex with three solid lines and a dashed arc separating two of them will indicate a variable number of edges. A line drawn initially solid and then dashed indicates that an edge may or may not be present. A solid line indicates that an edge is present. Examples of such diagrams are shown below in Figure 2.1.

Figure 2.1: Local diagrams of graphs. Vertex v on the left has at least 2 edges, vertex v_1 on the right has at least 1 edge, and vertex v_2 on the right has 1 or 2 edges.

Definition 2.0.3. A **weighted graph** is a pair (Γ, W), or just Γ, if W is understood, where Γ is a graph, and $W : V(\Gamma) \to \mathbb{Z}$ is a map from the vertices of Γ to the integers. W is called

the **weighting** of (Γ, W), and the integer $W(v)$ is called the **weight** of the vertex v. A **partially weighted graph** is the same as a weighted graph, but with the relaxed condition that the weighting need only be defined on a subset of the vertices. A diagram of a weighted graph is a diagram of the underlying graph with the weight of each vertex printed near the vertex.

Definition 2.0.4. Figure 2.2 shows a set of moves that locally transform one weighted graph to another. The portions of the weighted graphs not shown remain unchanged. These local moves will be referred to as **M1a**, **M1b**, **M1c**, **M2**, and **M3**, and their inverses as $\mathbf{M1a^{-1}}$, $\mathbf{M1b^{-1}}$, $\mathbf{M1c^{-1}}$, $\mathbf{M2^{-1}}$, and $\mathbf{M3^{-1}}$.

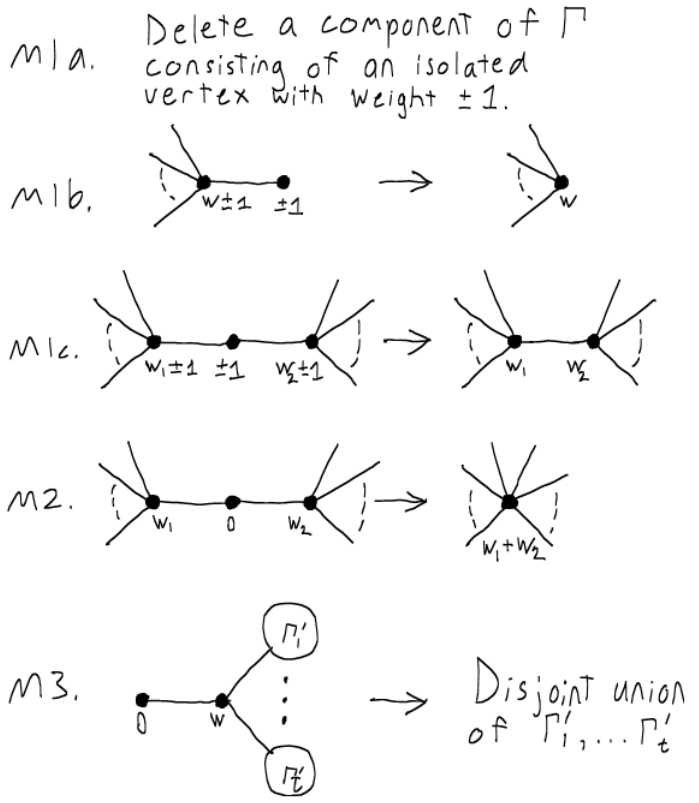

Figure 2.2: Weighted graph moves M1a, M1b, M1c, M2, and M3, which, together with their inverses, constitute a restricted form of the plumbing calculus from [8].

Remarks: The moves in Figure 2.2, together with their inverses, constitute a restricted form of the plumbing calculus from [8], which we will briefly discuss in Chapter 3. The reader should note that the application of move M1a, M1b, M1c, M2, or M3 requires a vertex weighted -1, 0, or 1 having valence 0, 1 or 2 to be present. Thus, if no such vertex

exists, none of those moves may be applied.

The transformation of a weighted graph under a move from {M1a,M1b,M1c} deleted one vertex, and then induces a natural bijective mapping on the rest of the vertices. This mapping preserves edges for all vertices except the one(s) adjacent to the deleted vertex. The change in edges for these adjacent vertices are clearly illustrated in Figure 2.2. Similar statements can be made for moves M2 or M3. For example, M2 deletes one vertex, and the induced mapping on vertices is 2-to-1 on the two vertices adjacent to the deleted vertex and injective on all the others. For all moves in {M1a,M1b,M1c,M2,M3}, the induced mappings on the non-deleted vertices are surjective.

Definition 2.0.5. Let Γ be a graph. A map $L : V(\Gamma) \to \{\text{E,F,e}\}$ from the set of vertices of Γ to the set of letters {E,F,e} is called a **pre-EFe-labeling** of Γ. $L(v)$ is called the **pre-EFe-label**, or just **label**, of v. If $L(v) = \text{E}$, then v is said to have label E, or v is E-labeled. Similar terminology holds if $L(v) = \text{F,e}$. Given a fixed pre-EFe-labeling L of Γ, we will define the functions **Eval**, **Fval**, **eval**, **val**: $V(\Gamma) \to \mathbb{Z}_{\geq 0}$ from the set of vertices of Γ to the nonnegative integers as follows: Eval(v) is equal to the number of edges in Γ that contain v, and whose vertex other than v is labeled E. Fval(v) is equal to the number of edges that contain v, and whose vertex other than v is labeled F. eval(v) is equal to the number of edges that contain v, and whose vertex other than v is labeled e. val is equal to Eval + Fval + eval, so val(v) is just the total number of edges containing v, i.e. its valence. Figure 2.3 shows a graph with labels printed near vertices. For this pre-EFe-labeling, Eval(v) = 2, Fval(v) = 1, and eval(v) = 2.

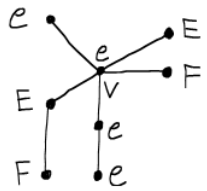

Figure 2.3: A diagram of a graph with a pre-EFe labeling. For this pre-EFe-labeling, Eval(v) = 2, Fval(v) = 1, and eval(v) = 2.

Definition 2.0.6. An **EFe-labeled graph** is a triple (Γ, W, L), or just Γ, if W and L are understood, where (Γ, W) is a weighted graph, and L is a pre-EFe-labeling of Γ such that every vertex $v \in V(\Gamma)$ satisfies the following properties:

If $L(v) = \text{E}$,

E1. $W(v) \geq \text{Eval}(v)$

E2. $\text{Eval}(v) + \text{Fval}(v) \leq 2$

If $L(v) = \text{F}$,

F1. $W(v) \leq -(\text{Fval}(v) + \text{eval}(v))$

If $L(v) = \text{e}$,

e1. $W(v) \leq -(1 + \text{Fval}(v))$

e2. $\text{val}(v) = 1$

e3. $\text{eval}(v) = 0$

L is then said to be an **EFe-labeling** of (Γ, W). A weighted graph (Γ, W) is said to "admit an EFe-labeling" if there exists a pre-EFe-labeling L of Γ such that L is an EFe-labeling of (Γ, W). A diagram of an EFe-labeled graph is a diagram of the underlying weighted graph with the label of each vertex printed near the vertex. Occasionally, if a vertex is assigned a letter variable as a name, that letter may be printed near the vertex, but it should be clear from the context whether this variable is the name of the vertex, the weight of the vertex, or the label of the vertex. Figure 2.4 below shows two diagrams of EFe-labeled graphs. The reader should check that the EFe-labels do indeed satisfy the properties outlined above.

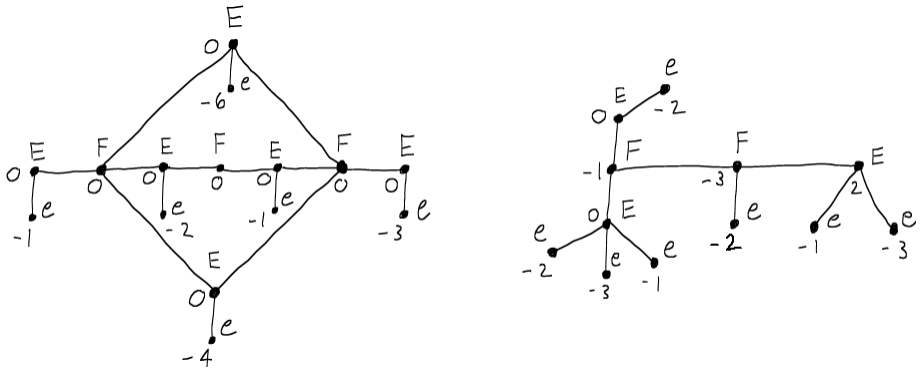

Figure 2.4: Two examples of EFe-labeled graphs.

Remarks: Notice that property E1 implies an E-labeled vertex has a nonnegative weight, property F1 implies an F-labeled vertex has a nonpositive weight, and property e1 implies an e-labeled vertex has a negative weight. Also notice the important fact that these defining properties are *local*; to check whether a vertex v of a pre-EFe-labeled graph satisfies the

EFe-labeled properties, the only information required is the label and weight of v, and the labels of those vertices that are connected to v by an edge. This fact allows an EFe-labeling of a graph Γ to descend to an EFe-labeling of a graph Γ' obtained from Γ by one of the local moves M1a, M1b, M1c, M2, or M3 shown in Figure 2.2. This is the content of the Theorem 2.0.7.

At this point, we pause for a brief digression to discuss the motivation for the EFe-labeling. In Definition 4.1.2, we define a weighted graph Γ constructed from a CW-complex C having underlying space the closed 2-disk. Such a CW-complex in the starting point for defining the cycle-free twisted face-pairing manifolds. The graph construction proceeds in three steps: Firstly, add one vertex to Γ for each edge and face of C, and weight these vertices 0. Secondly, add an edge to Γ connecting vertices v_1 and v_2 if v_1 corresponds to a face F of C, v_2 corresponds to an edge E of C, and F contains E. Thirdly, adjoin a single edge and vertex to each vertex of Γ that corresponds to an edge of C, and weight these new vertices with arbitrary negative integers. Figure 2.5 shows an example of such a construction.

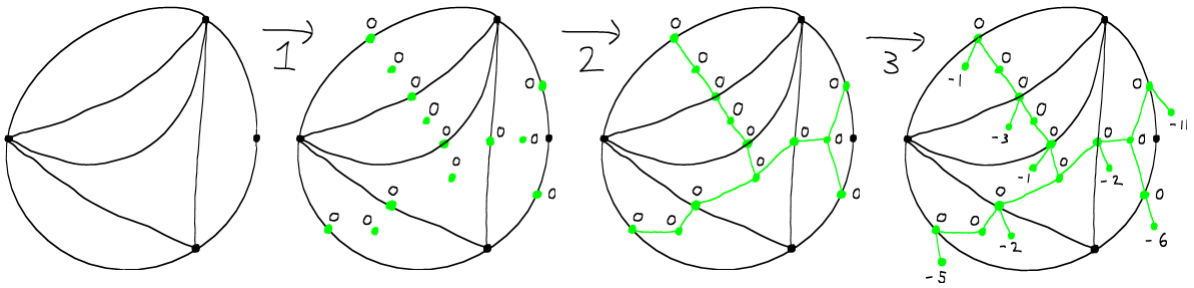

Figure 2.5: Construction of the weighted graph Γ from a CW-complex C with underlying space the closed 2-disk. C is drawn in black and Γ in green. The first step adds vertices weighted 0 to Γ for each edge and face of C. The second step adds an edge to Γ for each pair of vertices $\{v_1, v_2\}$ such that v_1 corresponds to a face F of C, v_2 corresponds to an edge E of C, and F contains E. The edge connects v_1 and v_2. The third step adjoins a single edge and vertex to each vertex of Γ that corresponds to an edge C, and weights these new vertices with arbitrary negative integers.

Γ admits the following EFe-labeling: The vertices of Γ corresponding to edges of C are labeled E. The vertices of Γ corresponding to faces of C are labeled F. The vertices of Γ added in step 3 are labeled e. This is the origin for the 'EFe' prefix in 'EFe-labeling'. The EFe-labeling for the example in Figure 2.5 is shown in Figure 2.6. The reader should check that Γ does indeed satisfy the properties of an EFe-labeled graph.

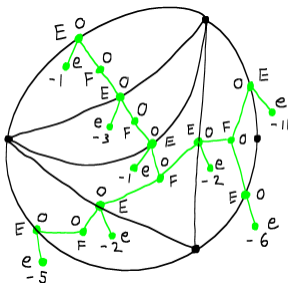

Figure 2.6: EFe-labeling of the graph Γ constructed from the CW-complex C. C is drawn in black and Γ in green.

Theorem 2.0.7. If a weighted graph (Γ, W) admits an EFe-labeling and (Γ', W') is a weighted graph obtained from (Γ, W) by any of the local moves M1a, M1b, M1c, M2, or M3 (but not their inverses) from Definition 2.0.4, then (Γ', W') admits an EFe-labeling.

Proof. Let (Γ, W) be a weighted graph and (Γ', W') a weighted graph related to (Γ, W) by one of the local moves from Definition 2.0.4. Let L be an EFe-labeling of (Γ, W). We will define a pre-EFe-labeling L' of Γ' and check that it is an EFe-labeling of (Γ', W'). Any vertex v of Γ *not* pictured in the local diagram on the left has a natural image vertex v' of Γ' *not* pictured in the local diagram on the right, as discussed in the remarks following Definition 2.0.4. Let $L'(v') = L(v)$. Then it remains to define L' for those vertices depicted on the right side of the local move.

Suppose the local move is M1a. Then there is no vertex in the local diagram on the right. The deletion of the isolated vertex does not affect the weights or labels of the remaining vertices, nor does it affect the values of the Eval, Fval, or eval functions on the remaining vertices. Then the L' labels of (Γ', W') trivially satisfy the EFe-labeling from Definition 2.0.6, since the L labels of (Γ, W) do.

Suppose the local move is M1b. Then there are 8 possibilities for the local weighting and EFe-labeling of Γ, and these are shown below in Figure 2.7 to the left of the arrows. We define the corresponding labeling L' of Γ' on the right.

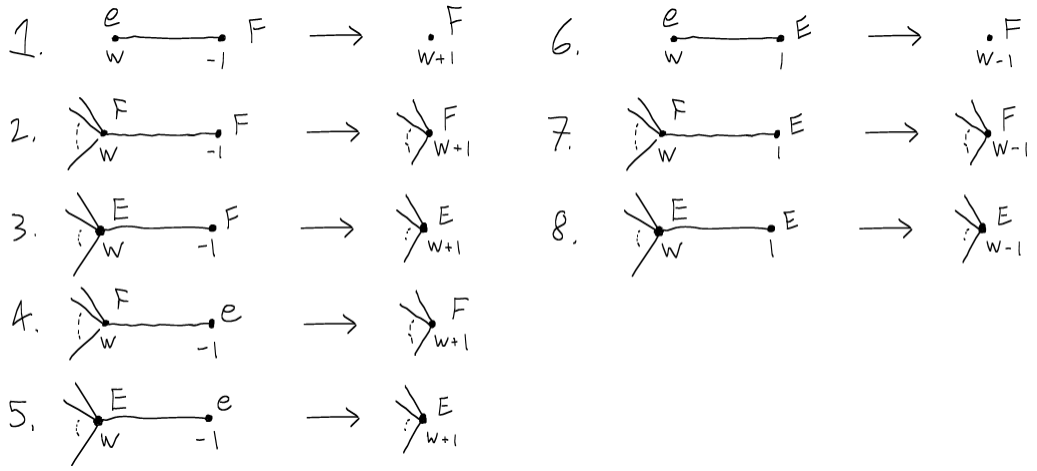

Figure 2.7: Weighted graphs transformed under the move M1b. The diagrams to the left of the arrows represent the 8 possible situations that can occur for an EFe-labeled graph, and the diagrams to the right of the arrows define an EFe-labeling of the transformed graphs.

The local diagrams to the left of the arrows are the only situations that can occur for Γ since the weight of any vertex labeled F or e is nonpositive by properties F1 and e1 from Definition 2.0.6, the weight of any vertex labeled E is nonnegative by E1, the e-valence of a vertex labeled e must be 0 by e2, and the valence of a vertex labeled e must be 1 by e3.

Now we will see that the diagrams on the right satisfy the properties of an EFe-labeling. The left vertices v in the local diagrams on the left correspond to the lone vertices v' in the local diagrams on the right.

Consider case 1. In this case, v has label e and weight w in (Γ, W, L), and $Fval(e) = 1$, so $w \leq -2$ by property e1 from Definition 2.0.6. v' has label F and weight $w+1$ in (Γ', W', L'). Then $w + 1 \leq -1 \leq 0$, and so property F1 of an F-labeled vertex is satisfied.

In case 2, v has label F and weight w in (Γ, W, L). Then $w \leq -(\text{Fval}(v) + \text{eval}(v))$ by property F1. v' has label F and weight $w + 1$ in (Γ', W', L'). The label of the vertices not shown in the local diagram remain the same, as L' was previously defined as such, so it follows that $\text{Fval}(v') = \text{Fval}(v) - 1$ and $\text{eval}(v') = \text{eval}(v)$. Then to see that v' satisfies property F1 of an F-labeled vertex, observe that

$$W'(v') = w+1 \leq -(\text{Fval}(v)+\text{eval}(v))+1 = -(\text{Fval}(v')+1+\text{eval}(v'))+1 = -(\text{Fval}(v')+\text{eval}(v'))$$

Finally, it can be seen that the L' labels of the local diagram of (Γ', W') were chosen so as to not change the values of the Eval, Fval, or eval functions on the vertices not shown; the

only changes were possible deletion of vertices or edges. Then the L' labels of these vertices not shown trivially satisfy the EFe-labeling conditions, since the L labels of (Γ, W) do.

In case 3, v has label E and weight w in (Γ, W, L). Then $w \geq \text{Eval}(v)$ by property E1 of Definition 2.0.6, and $\text{Eval}(v) + \text{Fval}(v) \leq 2$ by property E2. v' has label E and weight $w+1$ in (Γ', W', L'). The label of the vertices not shown in the local diagram remain the same, as L' was previously defined as such, so it follows that $\text{Fval}(v') = \text{Fval}(v) - 1$ and $\text{Eval}(v') = \text{Eval}(v)$. Then to see that v' satisfies the properties E1 and E2, observe that

$$W'(v') = w + 1 \geq w \geq \text{Eval}(v) = \text{Eval}(v')$$

$$\text{Eval}(v') + \text{Fval}(v') = \text{Eval}(v) + \text{Fval}(v) - 1 \leq 2 - 1 \leq 2$$

Finally, it can be seen that the L' labels of the local diagram of (Γ', W') were chosen so as to not change the values of the Eval, Fval, or eval functions on the vertices not shown; the only changes were possible deletion of vertices or edges. Then the L' labels of these vertices not shown trivially satisfy the EFe-labeling conditions, since the L labels of (Γ, W) do. Cases 4-8 can be checked similarly.

Now suppose the local move is M1c. Then there are 8 possibilities for the local weighting and EFe-labeling of Γ, and these are shown below in Figure 2.8 to the left of the arrows. We define the corresponding labeling L' of Γ' on the right.

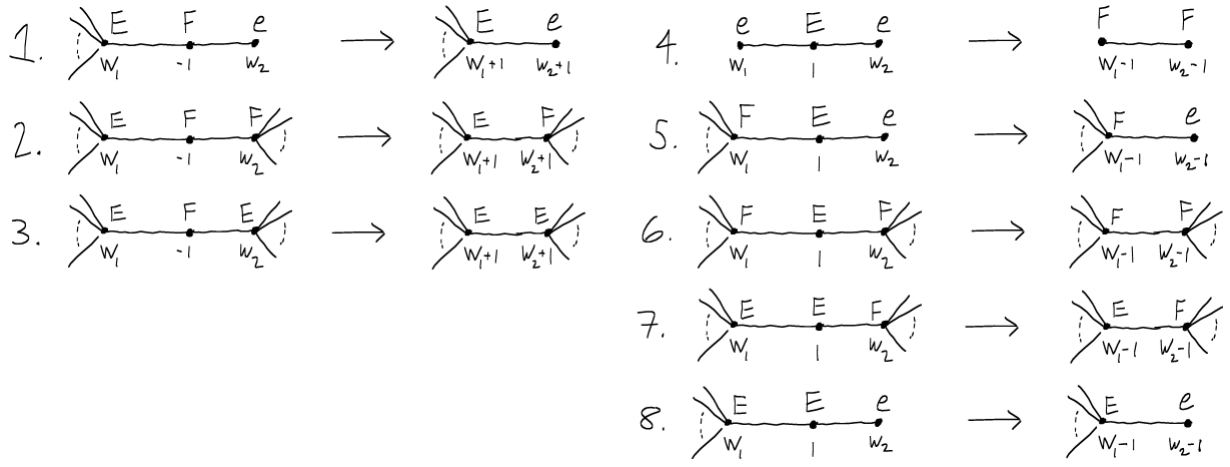

Figure 2.8: Weighted graphs transformed under the move M1c. The diagrams to the left of the arrows represent the 8 possible situations that can occur for an EFe-labeled graph, and the diagrams to the right of the arrows define EFe-labelings of the transformed graphs.

The local diagrams to the left of the arrows are the only situations that can occur for Γ for

the following reasons: a vertex weighted -1 must have label F or e since a vertex labeled E has nonnegative weight, by E1. A vertex weighted -1 with label F cannot be adjacent to two vertices labeled F, by F1. A vertex with valence 2 cannot be labeled e, by e2. A vertex weighted 1 with label E cannot be adjacent to two vertices labeled E, by E1.

Now we will see that the diagrams on the right satisfy the properties of an EFe-labeling. The left vertices v_1 and right vertices v_2 in the local diagrams on the left correspond to the left vertices v_1' and right vertices v_2' in the local diagrams on the right.

Consider case 1. In this case, v_1 has label E and weight w_1 and v_2 has label e and weight w_2 in (Γ, W, L). Then $w_1 \geq \text{Eval}(v_1)$ by property E1 from Definition 2.0.6, $\text{Eval}(v_1) + \text{Fval}(v_1) \leq 2$ by property E2, and $w_2 \leq -2$ by property e1. v_1' has label E and weight $w_1 + 1$ and v_2' has label e and weight $w_2 + 1$ in (Γ', W', L'). The label of the vertices not shown in the local diagram remain the same, as L' was previously defined as such, so it follows that $\text{Fval}(v_1') = \text{Fval}(v_1) - 1$ and $\text{Eval}(v_1') = \text{Eval}(v_1)$. Then to see that v_1' satisfies the properties E1 and E2, observe that

$$W'(v_1') = w_1 + 1 \geq w_1 \geq \text{Eval}(v_1) = \text{Eval}(v_1')$$

$$\text{Eval}(v_1') + \text{Fval}(v_1') = \text{Eval}(v_1) + \text{Fval}(v_1) - 1 \leq 2 - 1 \leq 2$$

To see that v_2' satisfies the properties of an e-labeled vertex, observe that

$$W'(v_2') = w_2 + 1 \leq -2 + 1 = -1 = -(1 + \text{Fval}(v_2'))$$

$$\text{val}(v_2') = 1$$

$$\text{eval}(v_2') = 0$$

Finally, it can be seen that the L' labels of the local diagram of (Γ', W') were chosen so as to not change the values of the Eval, Fval, or eval functions on the vertices not shown; the only changes were possible deletion of vertices or edges. Then the L' labels of these vertices not shown trivially satisfy the EFe-labeling conditions, since the L labels of (Γ, W) do.

In case 7, v_1 has label E and weight w_1 and v_2 has label F and weight w_2 in (Γ, W, L). Then $w_1 \geq \text{Eval}(v_1)$ by property E1 from Definition 2.0.6, $\text{Eval}(v_1) + \text{Fval}(v_1) \leq 2$ by property E2, and $w_2 \leq -(\text{Fval}(v_2) + \text{eval}(v_2))$ by property F1. v_1' has label E and weight $w_1 - 1$ and v_2' has label F and weight $w_2 - 1$ in (Γ', W', L'). The label of the vertices not shown in the local diagram remain the same, as L' was previously defined as such, so it follows that $\text{Fval}(v_1') = \text{Fval}(v_1) + 1$, $\text{Eval}(v_1') = \text{Eval}(v_1) - 1$, $\text{Fval}(v_2') = \text{Fval}(v_2)$, $\text{Eval}(v_2') = \text{Eval}(v_2)$, and $\text{eval}(v_2') = \text{eval}(v_2)$. Then to see that v_1' satisfies E1 and E2, observe that

$$W'(v_1') = w_1 - 1 \geq \text{Eval}(v_1) - 1 = \text{Eval}(v_1')$$

$$\text{Eval}(v_1') + \text{Fval}(v_1') = \text{Eval}(v_1) - 1 + \text{Fval}(v_1) + 1 = \text{Eval}(v_1) + \text{Fval}(v_1) \leq 2$$

To see that v_2' satisfies property F1, observe that

$$W'(v_2') = w_2 - 1 \leq w_2 \leq -(\text{Fval}(v_2) + \text{eval}(v_2)) = -(\text{Fval}(v_2') + \text{eval}(v_2'))$$

Finally, it can be seen that the L' labels of the local diagram of (Γ', W') were chosen so as to not change the values of the Eval, Fval, or eval functions on the vertices not shown; the only changes were possible deletion of vertices or edges. Then the L' labels of these vertices not shown trivially satisfy the EFe-labeling conditions, since the L labels of (Γ, W) do. Cases 2-6,8 can be checked similarly.

Next, suppose the local move is M2. Then there are 4 possibilities for the local weighting and EFe-labeling of Γ, and these are shown below in Figure 2.9 to the left of the arrows. We define the corresponding labeling L' of Γ' on the right.

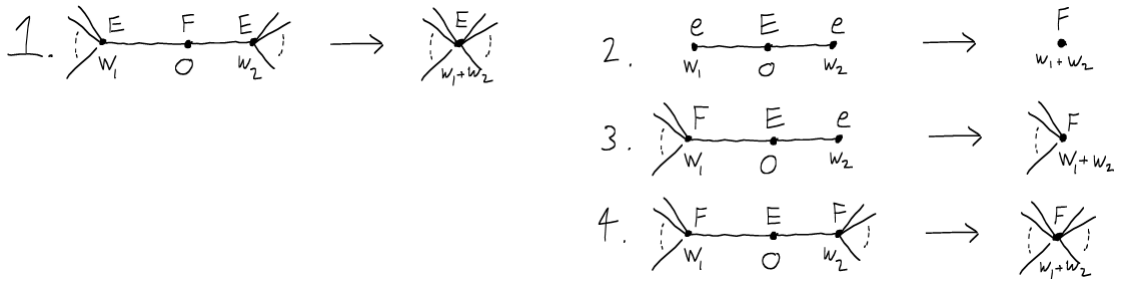

Figure 2.9: Weighted graphs transformed under the move M2. The diagrams to the left of the arrows represent the 4 possible situations that can occur for an EFe-labeled graph, and the diagrams to the right of the arrows define EFe-labelings of the transformed graphs.

The local diagrams to the left of the arrows are the only situations that can occur for Γ for the following reasons: A vertex labeled e cannot have weight 0, by property e1. If a vertex labeled F has weight 0, it cannot be adjacent to any vertex labeled F or e, by F1. If a vertex labeled E has weight 0, it cannot be adjacent to a vertex labeled E, by E1.

Now we will see that the diagrams on the right satisfy the properties of an EFe-labeling. The left vertices v_1 and right vertices v_2 in the local diagrams on the left correspond to the lone vertex v' in the local diagram on the right.

Consider case 1. In this case, v_1 has label E and weight w_1 and v_2 has label E and weight w_2 in (Γ, W, L). Then $w_1 \geq \text{Eval}(v_1)$ by property E1 from Definition 2.0.6, $\text{Eval}(v_1) + \text{Fval}(v_1) \leq 2$ by property E2, $w_2 \geq \text{Eval}(v_2)$ by property E1, and $\text{Eval}(v_2) + \text{Fval}(v_2) \leq 2$

by property E2. v' has label E and weight $w_1 + w_2$ in (Γ', W', L'). The label of the vertices not shown in the local diagram remain the same, as L' was previously defined as such, so it follows that $\text{Fval}(v') = \text{Fval}(v_1) + \text{Fval}(v_2) - 2$ and $\text{Eval}(v') = \text{Eval}(v_1) + \text{Eval}(v_2)$. Then to see that v' satisfies the properties E1 and E2, observe that

$$W'(v') = w_1 + w_2 \geq \text{Eval}(v_1) + \text{Eval}(v_2) = \text{Eval}(v')$$

$$\text{Eval}(v') + \text{Fval}(v') = \text{Eval}(v_1) + \text{Eval}(v_2) + \text{Fval}(v_1) + \text{Fval}(v_2) - 2 \leq 4 - 2 = 2$$

Finally, it can be seen that the L' labels of the local diagram of (Γ', W') were chosen so as to not change the values of the Eval, Fval, or eval functions on the vertices not shown; the only changes were possible deletion of vertices or edges. Then the L' labels of these vertices not shown trivially satisfy the EFe-labeling conditions, since the L labels of (Γ, W) do.

In case 4, v_1 has label F and weight w_1 and v_2 has label F and weight w_2 in (Γ, W, L). Then $w_1 \leq -(\text{Fval}(v_1) + \text{eval}(v_1))$ by property F1 from Definition 2.0.6, and $w_2 \leq -(\text{Fval}(v_2) + \text{eval}(v_2))$ by property F1. v' has label F and weight $w_1 + w_2$ in (Γ', W', L'). The label of the vertices not shown in the local diagram remain the same, as L' was previously defined as such, so it follows that $\text{Fval}(v') = \text{Fval}(v_1) + \text{Fval}(v_2)$ and $\text{eval}(v') = \text{eval}(v_1) + \text{eval}(v_2)$. Then to see that v' satisfies the property F1, observe that

$$W'(v') = w_1 + w_2 \leq -(\text{Fval}(v_1) + \text{eval}(v_1)) - (\text{Fval}(v_2) + \text{eval}(v_2)) = -(\text{Fval}(v') + \text{eval}(v'))$$

Finally, it can be seen that the L' labels of the local diagram of (Γ', W') were chosen so as to not change the values of the Eval, Fval, or eval functions on the vertices not shown; the only changes were possible deletion of vertices or edges. Then the L' labels of these vertices not shown trivially satisfy the EFe-labeling conditions, since the L labels of (Γ, W) do. Cases 2-3 can be checked similarly.

Finally, suppose the local move is M3. Then no vertex is shown in the diagram on the right. The label of the vertices not shown on the right are the same as the corresponding ones on the left, as L' was previously defined this way. Then local move M3 only decreases the Eval, Fval, or eval of some of the vertices, each by at most one. Since the vertices not shown on the left satisfied the EFe-labeling conditions, the corresponding vertices on the right do also, since a decrease in Eval, Fval, or eval will not violate any properties from Definition 2.0.6. The only exception to this is that a vertex labeled e may change from having total valence 1 to total valence 0, in which case it becomes an isolated vertex, and this will violate property e2. This situation is fixed by changing the label of this isolated vertex from e to F. Q.E.D.

Remarks: As remarked earlier, the set of moves
$\{\text{M1a,M1b,M1c,M2,M3,M1a}^{-1}\text{,M1b}^{-1}\text{,M1c}^{-1}\text{,M2}^{-1}\text{,M3}^{-1}\}$ constitutes a restricted form of

the plumbing calculus from [8]. Theorem 2.0.7 can then be viewed as stating that the admittance of an EFe-labeling is semi-invariant under the plumbing calculus, since it is invariant under moves from {M1a,M1b,M1c,M2,M3} but not necessarily moves from {M1a^{-1},M1b^{-1},M1c^{-1},M2^{-1},M3^{-1}}.

Chapter 3

EFe-Labeled Graphs and Their Plumbed Manifolds

In Chapter 2, we defined weighted graphs. In this chapter, we begin with Definition 3.1.2, which assigns to each weighted graph which is a forest a closed, connected, oriented 3-manifold. The manifold is said to be 'plumbed' from the weighted graph. Any 3-manifold homeomorphic to a manifold plumbed from a weighted graph is called a graph manifold. Graph manifolds were first introduced by Waldhausen in [12]. Actually, the graph manifolds he considered are more general than the ones arising from weighted forests, which form a proper subclass of the graph manifolds.

Theorem 4.2.3 gives us a strong relationship between cycle-free twisted face-pairing manifolds and plumbed manifolds, so the theory of plumbed manifolds developed in this chapter becomes instrumental in our understanding of cycle-free twisted face-pairing manifolds.

3.1 Plumbed Manifolds, Plumbing Graphs and Their Normal Forms

Definition 3.1.1. A **tree** is a connected graph without cycles. If each connected component of a graph is a tree, the graph is called a **forest**. A **weighted forest** (resp., **weighted tree**) is a weighted graph (Γ, W) where Γ is a forest (resp., tree).

Definition 3.1.2. Define $\boldsymbol{N(\Gamma, W)}$ to be the plumbed oriented 3-manifold from the weighted forest (Γ, W). The definition of plumbed 3-manifolds is given in Section 1.1.3 on page 12 of [10]. (Γ, W) is said to be a **plumbing graph** for $N(\Gamma, W)$. Plumbed 3-manifolds only arise

in Theorems 3.1.3 and 4.2.3, and the proof of these theorems are cited from other texts. Thus, we omit the details of this definition here.

Theorem 3.1.3. Two plumbed manifolds $N(\Gamma, W)$ and $N(\Gamma', W')$ are orientation-preservingly homeomorphic if and only if (Γ, W) can be related to (Γ', W') by a sequence of the moves from Definition 2.0.4 and their inverses.

Proof. This is precisely Proposition 2.2 from [7].

Remarks: In [8], Neumann describes the full plumbing calculus which consists of a set of moves that transform general plumbing graphs. These are the plumbing graphs giving rise to the full class of graph manifolds. The weighted forests of Definition 3.1.1 constitute a subclass of the plumbing graphs, and the local moves of Definition 2.0.4 constitute the restriction to weighted forests of a subset of the plumbing calculus moves. Theorem 3.1.3 can now be viewed as stating that this subset of moves is a sufficient calculus when restricted to the weighted forests.

Definition 3.1.4. A **chain** of a graph is a nonempty, connected subgraph in which every vertex has valence 0, 1, or 2 in the original graph. A **maximal chain** of a graph is a chain that is not properly contained in another chain. The **length** of a chain is the number of vertices it contains. A **terminal vertex** of a chain is a vertex that is not contained in a chain but is connected to a vertex in a chain by an edge. Examples of these are shown below in Figure 3.1.

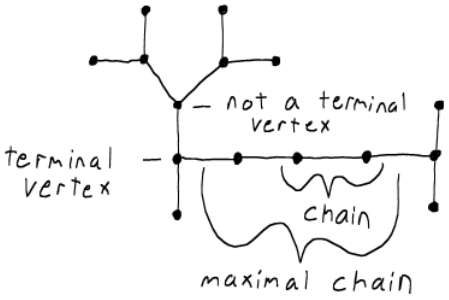

Figure 3.1: Diagram of a graph. The graph has 1 maxmial chain of length 3, 7 maximal chains of length 1, and 4 terminal vertices.

Definition 3.1.5. For each weighted graph (Γ, W), define a partially weighted graph by collapsing each maximal chain of Γ to a single vertex without a weight, removing the weights of terminal vertices, and leaving the weights of non-terminal and non-chain vertices unchanged. This new partially weighted graph is called the **quotient by maximal chains** of (Γ, W). If two weighted graphs have the same quotient by maximal chains, they are called **equivalent**

modulo maximal chains. It is immediate that this is an equivalence relation on the class of weighed graphs. Two equivalent weighted graphs, and their common partially weighted quotient graph, are shown below in Figure 3.2.

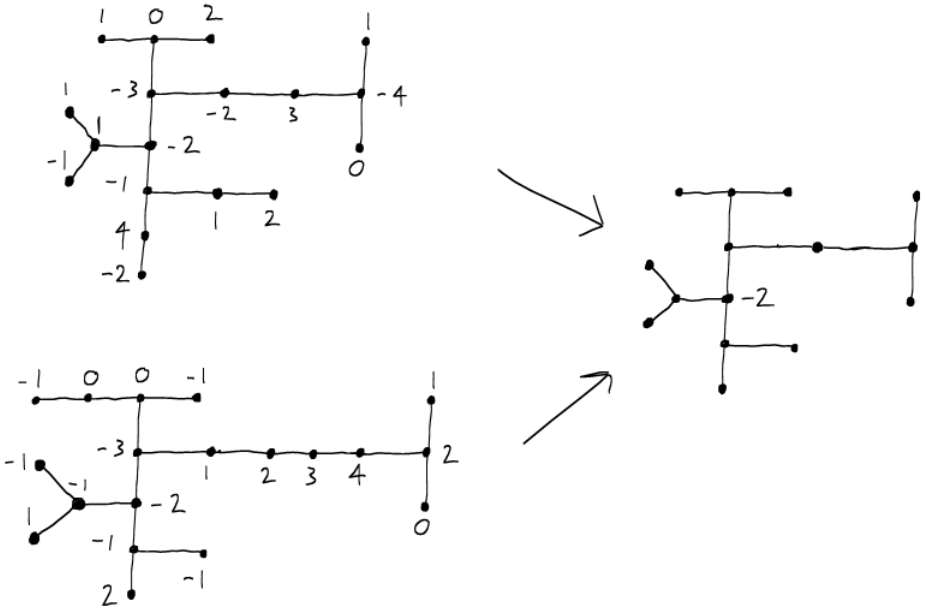

Figure 3.2: Two weighted graphs that are equivalent modulo maximal chains are shown on the left. Their common partially weighted quotient graph is shown on the right.

Definition 3.1.6. A weighted tree is said to be in **subnormal form** if no sequence of moves from {M1a,M1b,M1c,M2,M3} shown in Figure 2.2 can be applied to it. A weighted tree is said to be in **normal form** if it consists of a single vertex weighted 0 (in which case it is also in subnormal form), or it is in subnormal form and every vertex contained in a chain has weight at most -2. A weighted forest is said to be in subnormal form if each of its component trees are in subnormal form, and in normal form if each of its component trees are in normal form.

Theorem 3.1.7. Every weighted forest can be transformed to a weighted forest in normal form by a sequence of moves from Figure 2.2 and their inverses. Moreover, the transformation can be achieved by an algorithm that first brings the graph to subnormal form by applying moves only from {M1a,M1b,M1c,M2,M3} and not their inverses, and then applying moves from {M1b,M1b^{-1},M1c,M1c^{-1}} while leaving the quotient of the graph by maximal chains unchanged.

Proof. The existence of a normal form for a weighted forest follows from Theorem 4.1 from [8], and we outline the algorithm for transforming the graph to normal form here. First

apply any sequence of moves from {M1a,M1b,M1c,M2,M3} until none further can be made. This sequence must terminate since each move involves the deletion of at least one vertex, and the graph involved is finite. The graph is now in subnormal form, and so this completes the first step of the algorithm.

For the second step, we will focus on a single component tree, and prove that it can be brought to normal form by a sequence of moves from {M1b,M1b^{-1},M1c,M1c^{-1}} that leave the quotient by maximal chains unchanged. If this component is a single vertex weighted 0, then it is already in normal form, so we may assume that the component is not a single vertex weighted 0. The proof will be by induction on n, the number of vertices lying in a chain of the component with weight greater than -2.

Since no move from {M1a,M1b,M1c,M2,M3} can be applied to the component, and since the component does not consist of a single vertex weighted 0, no vertex in a chain with weight greater than -2 can have weight -1, 0, or 1 (or else one of those moves could be applied), so it suffices to consider vertices lying in chains with weights greater than or equal to 2. The base case $n = 0$ is trivial, since in this case the component is already in normal form, and so no moves need be applied. Assume that, for some $n \in \mathbb{N}$, whenever there exist less than or equal to n vertices with weights at least 2 lying in chains in a connected weighted graph in subnormal form, there exists a sequence of moves from {M1b,M1b^{-1},M1c,M1c^{-1}} transforming it to normal form which leaves the quotient of the graph by maximal chains unchanged. Now suppose we have a connected weighted graph in subnormal form having $n + 1$ vertices lying in chains with weights at least 2. We shall focus on one such vertex v with weight w and describe a sequence of moves. Since v lies in a chain, it has valence 0, 1, or 2. We will treat the case $\mathrm{val}(v) = 2$ here, and the cases $\mathrm{val}(v) = 0, 1$ can be shown from a similar argument. Apply move M1c^{-1} $w - 1$ times, and then move M1c as indicated below in Figure 3.3. The result of this sequence is to replace v with a chain of length $w - 1$, each vertex contained within having weight -2, and to subtract 1 from the weights of the two vertices adjacent to v. These moves at most affect the length of a chain and the weights of vertices in a chain or terminal vertices, and such changes do not affect the quotient of the graph by maximal chains.

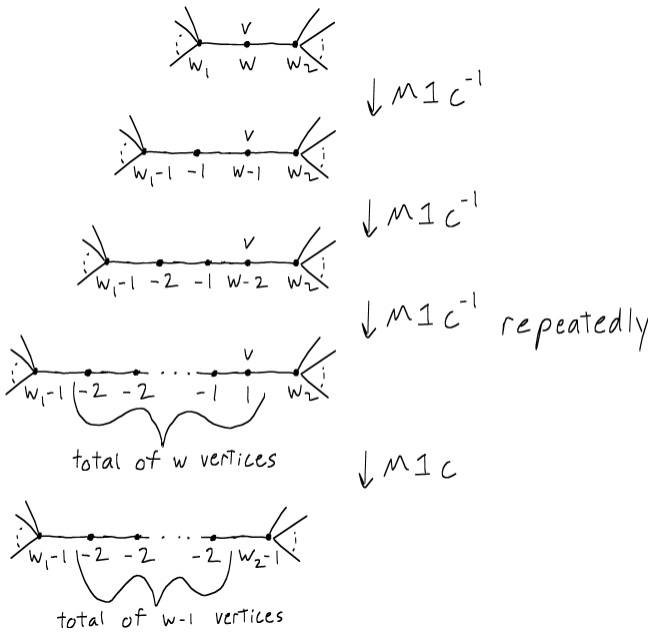

Figure 3.3: A sequence of moves applied to the weighted graph to remove the vertex v having weight $w \geq 2$.

Now there are at most n vertices lying in chains with weights greater than or equal to 2. But to use the inductive hypothesis, the current graph must be in subnormal form. This may no longer be true, precisely if the vertex weighted w_1 or the vertex weighted w_2 in Figure 3.3 has weight 2 and valence 1 or 2, since in this case there will now be a vertex with weight 1 lying in a chain. We will treat the case $w_1 = 2$, and the same argument applies for the case $w_2 = 2$. This situation is shown in the first two diagrams of Figure 3.4. Suppose that there is a maximum of m consecutive vertices of weight 2 adjacent to v and lying in a chain. Then these m vertices themselves form a chain. The last vertex in this chain may have valence 1 or 2. We will treat the case that the valence is 2, and the other case follows from a similar argument. It follows by induction on m that applying move M1c m times deletes this chain, subtracts m from the weight of one adjacent vertex, and subtracts 1 from the weight of the other adjacent vertex. This step is shown in the last diagram in Figure 3.4.

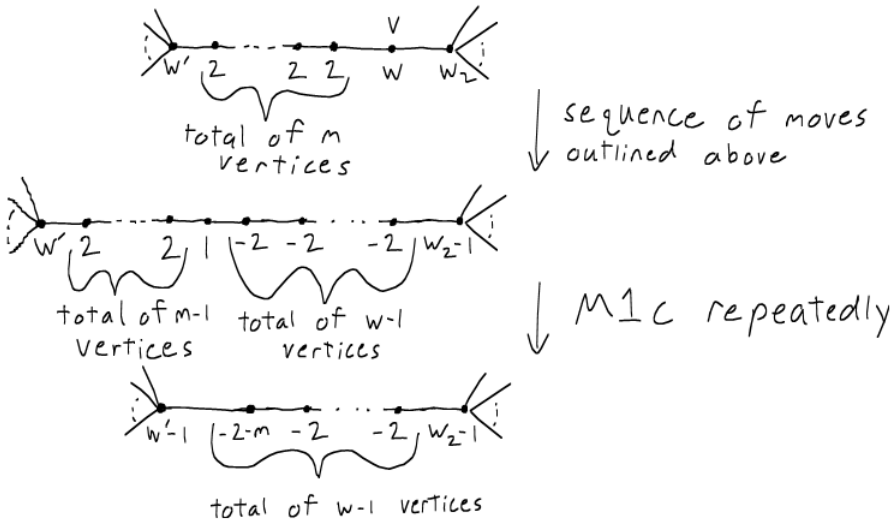

Figure 3.4: Removing a chain of vertices with weights 2 by repeated application of move M1c.

Again, throughout this process, only moves from {M1b,M1b^{-1},M1c,M1c^{-1}} are used, and the quotient of the graph by maximal chains remains unchanged. It is now that case that the graph is in subnormal form since either the vertex weighted w' in Figure 3.4 does not lie in the chain, $w' - 1 \geq 2$, or $w' - 1 \leq -3$. Furthermore, there are precisely $n - m$ vertices lying in chains with weights greater than or equal to 2. Then by the inductive hypothesis, there exists a sequence of moves from {M1b,M1b^{-1},M1c,M1c^{-1}} bringing the graph to normal form and leaving the quotient of the graph by maximal chains unchanged. This completes the inductive step and proof of the existence of the algorithm. Q.E.D.

Theorem 3.1.8. If (Γ_1, W_1) and (Γ_2, W_2) are two graphs in normal form such that $N(\Gamma_1, W_1)$ and $N(\Gamma_2, W_2)$ are homeomorphic to the same Seifert fibered space over S^2 having normalized invariants $\{Oo0\big|b; (\alpha_1, \beta_1), \ldots (\alpha_n, \beta_n)\}$ with $n \geq 3$, then $(\Gamma_1, W_1) = (\Gamma_2, W_2)$.

Remarks: The definition for normal form for a weighted graph we give in Definition 3.1.6 is similar to the normal form definition of Neumann in Section 4 of [8]. To avoid confusion, we will refer to the normal form of Definition 3.1.6 as G-normal form, and that from [8] as N-normal form in these remarks and the proof following. The reason we introduce N-normal forms is that they not only exist but are unique, by Theorem 4.2 from [8], and we will use this fact to obtain our desired uniqueness result. The reader may wonder why we did not just make the N-normal form our definition of normal form in the first place. The reason is that the graphs considered in [8] are allowed to have more decorations than just integer weights on vertices, and, correspondingly, the set of local moves transforming the graphs

is strictly larger than the set of moves from Definition 2.0.4. The manifolds plumbed from these graphs are the graph manifolds, and the set of local moves makes up the full plumbing calculus. We do not need such generality in this paper.

Proof. The list of conditions we give for G-normal forms in Definition 3.1.6 is a subset of the conditions for N-normal forms, so a graph in N-normal form is also in G-normal form. However, a graph in G-normal form will fail to be in N-normal form precisely when a local diagram of the graph has the form shown in Figure 3.5, because the graph will then violate condition N3 on pages 311-312 from [8].

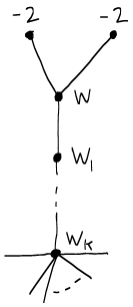

Figure 3.5: Local diagram of a graph in G-normal form but not N-normal form.

If this situation occurs for a particular graph, then the transformation that brings the graph to N-normal form adds an extra decoration to one of the vertices. Two examples of this are shown in Figure 3.6. The extra decorations are the negative integers in brackets.

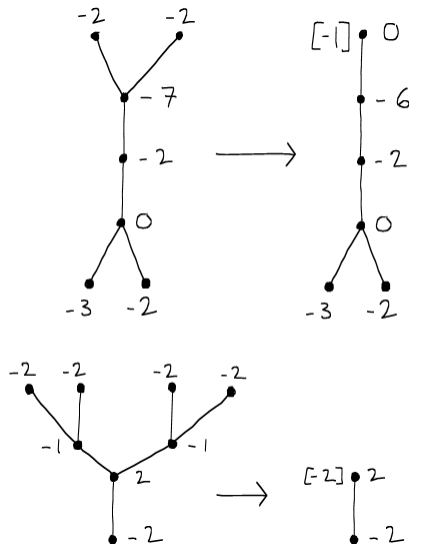

Figure 3.6: Example of transforming graphs that violate condition N3 from [8] into N-normal form graphs. The graphs in N-normal form all have a vertex decorated with a negative integer in brackets.

Thus, at this point, we can say that there are two mutually exclusive alternatives for any graph in G-normal form: 1) The graph is in N-normal form. 2) The graph is not in N-normal form and its N-normal form graph contains a vertex decorated with a negative integer in brackets.

Now suppose we have two graphs (Γ_1, W_1) and (Γ_2, W_2) in G-normal form as in the statement of the theorem. Since their plumbed manifold is Seifert fibered over S^2 with $n \geq 3$, it follows from Corollary 5.7 in [8] that the N-normal form of these graphs does not have any vertices decorated with a negative integer in brackets. Then the graphs do not satisfy the second of our alternatives, so they must be in N-normal form. By uniqueness of N-normal forms from Theorem 4.2 in [8], we must have $(\Gamma_1, W_1) = (\Gamma_2, W_2)$. Q.E.D.

3.2 Seifert Fibered Spaces Plumbed from EFe-Labeled Graphs

Theorem 3.2.1. An oriented Seifert fibered space over S^2 with invariants

$\{Oo0\big|b; (\alpha_1, \beta_1), \ldots (\alpha_n, \beta_n)\}$ is orientation-preservingly homeomorphic to the plumbed manifold of the weighted tree shown below in Figure 3.7.

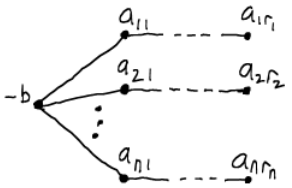

Figure 3.7: Plumbing graph for the Seifert fibered manifold with invariants $\{Oo0\big|b; (\alpha_1, \beta_1), \ldots (\alpha_n, \beta_n)\}$.

In Figure 3.7, $\{a_{ij}\}$ are integers such that $[a_{i1}, \ldots a_{ir_i}] = \dfrac{\alpha_i}{\beta_i}$. The bracket notation means continued fraction. Figure 3.8 shows the continued fraction equal to $[z_1, \ldots z_n]$.

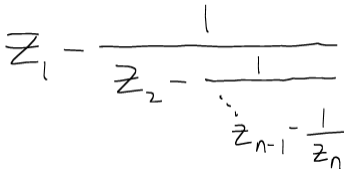

Figure 3.8: Continued fraction equal to $[z_1, \ldots z_n]$.

Proof. This is stated in the second paragraph of the proof of Proposition 3.3 from [7].

Corollary 3.2.2. An oriented Seifert fibered space over S^2 having normalized invariants $\{Oo0\big|b; (\alpha_1, \beta_1), \ldots (\alpha_n, \beta_n)\}$ with $n \geq 3$ is orientation-preservingly homeomorphic to the plumbed manifold of the weighted tree in normal form with local diagram shown below in Figure 3.9 where $w_i \leq -2$ for each $i \leq n$ (note that if $n < 3$, the graph may not be in normal form since the central vertex weighted $-b-n$ will belong to a chain). The rest of the diagram not shown consists of n chains containing vertices with weights less than or equal to -2. Here, the invariants being normalized means $0 < \beta_i < \alpha_i$ for all i.

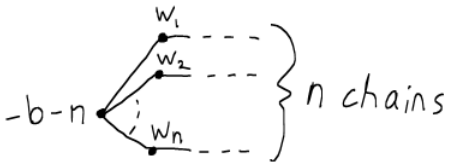

Figure 3.9: Local diagram of the normal form of the weighted graph representing the Seifert fibered space with normalized invariants $\{Oo0\big|b; (\alpha_1, \beta_1), \ldots (\alpha_n, \beta_n)\}$. $w_i \leq -2$ for each $i \leq n$.

Proof. The Seifert fibered space is orientation-preservingly homeomorphic to the plumbed manifold shown in Figure 3.7 by Theorem 3.2.1. Since the invariants are normalized, $\frac{\alpha_i}{\beta_i} > 1$ for all i. This implies that the integers $\{a_{ij}\}$ in Figure 3.7 satisfying $[a_{i1}, \ldots a_{ir_i}] = \frac{\alpha_i}{\beta_i}$ can be chosen to all be at least 2, and we choose so here. The graph in Figure 3.7 will then be in subnormal form, since all the vertices having valence at most 2 have weight at least 2 (since $n \geq 3$, the central vertex weighted $-b$ does not lie in a chain). Now we follow the algorithm in Theorem 3.1.7, and bring the graph in Figure 3.7 to normal form by a sequence of moves from {M1b,M1b^{-1},M1c,M1c^{-1}} that leaves the quotient of the graph by maximal chains unchanged. Since $a_{11} \geq 2$, we must remove the vertex weighted a_{11} by replacing it with a chain of length $a_{11} - 1$, each of whose vertices has weight -2. We also subtract 1 from the one or two vertices adjacent to the one weighted a_{11} as a result of this process. This is shown in Figure 3.10.

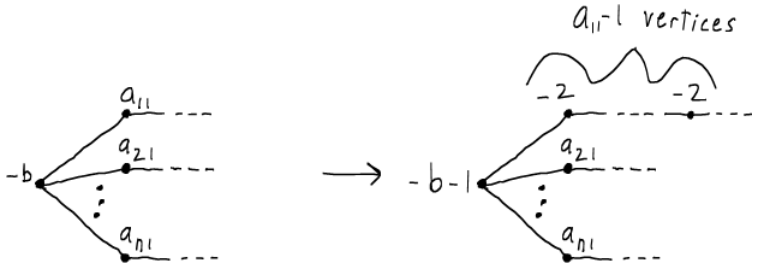

Figure 3.10: Process of removing vertices weighted a_{11} by replacing it with a chain of vertices weighted -2.

From here, we continue applying moves from {M1b,M1b^{-1},M1c,M1c^{-1}} to the first chain until every vertex belonging to it has weight at most -2. But none of those vertices is connected to the central vertex by an edge, so at the end of this process, it still has weight $-b-1$, and the vertex adjacent to it in the first chain has weight w_1 for some $w_1 \leq -2$. We repeat this exact same process to the second chain, which first subtracts 1 from the weight of the central vertex (so it now has weight $-b-2$) and then does not change its weight again. The central vertex will then be adjacent to a vertex in the second chain weighted w_2 for some $w_2 \leq -2$. We continue in this way for each of the n chains, which finally results in the graph shown in Figure 3.9, where the central vertex has weight $-b-n$, and $w_i \leq -2$ for each $i \leq n$. Q.E.D.

The next theorem, Theorem 3.2.3, is one of the major ingredients (along with Theorems 4.1.3 and 4.2.3) in the proof of one of the main results this paper, Theorem 5.1.1. It states that weighted graphs whose plumbed manifolds are Seifert fibered spaces with certain normalized invariants cannot admit an EFe-labeling. The class of manifolds we are interested in for

this paper, the cycle-free twisted face-pairing manifolds, which will be defined in Chapter 4, *always* can be plumbed from weighted graphs admitting an EFe-labeling. This is essentially the content of Theorem 4.1.3. So then Theorems 3.2.3 and 4.1.3 should be seen as the motivation for defining EFe-labeling.

Theorem 3.2.3. If M is an oriented Seifert fibered space over S^2 with normalized invariants $\{Oo0\big|b; (\alpha_1, \beta_1), \ldots (\alpha_n, \beta_n)\}$ such that $n \geq 3$ and $-n < b < 0$, then M is not orientation-preservingly homeomorphic to $N(\Gamma, W)$ for any weighted forest (Γ, W) admitting an EFe-labeling.

Remarks: Before beginning the proof, we open with remarks that hopefully explain the necessity for the methods used. In Figure 3.9 from Corollary 3.2.2, we have a diagram of a weighted graph (Γ', W') in normal form whose plumbed manifold is M, the Seifert fibered space in the statement of this theorem. We can readily check that (Γ', W') does not admit an EFe-labeling. If we have any other weighted graph (Γ, W) whose plumbed manifold is M, then by Theorem 3.1.3, (Γ, W) is related to (Γ', W') by a sequence of moves Figure 2.2 *and their inverses*. If we knew that the admittance of an EFe-labeling was invariant under those moves *and their inverses*, then we would know that (Γ, W) does not admit an EFe-labeling since (Γ', W') doesn't, and the theorem would be proved. But Theorem 2.0.7 only guarantees that the admittance of an EFe-labeling is invariant under moves from Figure 2.2 *and not necessarily their inverses*. This makes the proof more difficult, and necessitates the use of the full force of the Theorems 3.1.7 and 3.1.8.

Proof. Let M be an oriented Seifert fibered space over S^2 with normalized invariants $\{Oo0\big|b; (\alpha_1, \beta_1), \ldots (\alpha_n, \beta_n)\}$ such that $n \geq 3$ and $-n < b < 0$, and assume there exists a weighted forest (Γ, W) admitting an EFe-labeling such that M is orientation-preservingly homeomorphic to $N(\Gamma, W)$. We now follow the algorithm of Theorem 3.1.7 that brings (Γ, W) to normal form. First, apply any sequence of moves from {M1a,M1b,M1c,M2,M3} in Figure 2.0.4, but not their inverses, until no further move may be applied, and call the resulting weighted graph (Γ', W'), which is in subnormal form. We will show that (Γ', W') must take a certain form.

Since (Γ', W') is in subnormal form, it can be brought to normal form by moves that do not change its quotient by maximal chains, by Theorem 3.1.7. Since $N(\Gamma', W') \approx N(\Gamma, W) \approx M$, the normal form of (Γ', W') is unique by Theorem 3.1.8, so the normal form must be that shown in Figure 3.9. So then (Γ', W') can be transformed to the graph in Figure 3.9 by moves that do not change its quotient by maximal changes. The two graphs are then equivalent modulo maximal chains. This means that the quotient of (Γ', W') is exactly of the form in Figure 3.11.

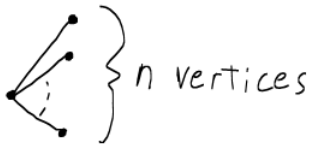

Figure 3.11: The quotient of (Γ', W') by maximal chains.

This in turn implies that (Γ', W') has a local diagram shown in Figure 3.12, for some integers $c, w_1, \ldots w_n$, by expanding those vertices back into chains.

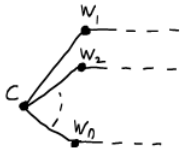

Figure 3.12: Local diagram of (Γ', W').

We will try to derive more information about these integers. Since (Γ', W') is in subnormal form, we must have $w_i \leq -2$ or $w_i \geq 2$ for each i, or else one of M1b, M1c, M2, or M3 could be applied. Let s be the total number of integers from $w_1, \ldots w_n$ that are negative. After reindexing, we may assume that (Γ', W') has local diagram shown in Figure 3.13, where $w_i \leq -2$ for $i \leq s$, and $w_i \geq 2$ for $i \geq s+1$.

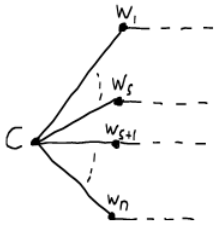

Figure 3.13: Local diagram of (Γ', W'). $w_i \leq -2$ for $i \leq s$, and $w_i \geq 2$ for $i \geq s+1$

Now we follow the second step of the algorithm in Theorem 3.1.7 for bringing (Γ', W') to normal form, by performing a sequence of moves from $\{\text{M1b}, \text{M1b}^{-1}, \text{M1c}, \text{M1c}^{-1}\}$ to remove the vertices lying in chains with positive weights. In this case, that includes the vertices weighted w_i for $s+1 \leq i \leq n$. The result of applying these moves for those vertices is shown below in Figure 3.14.

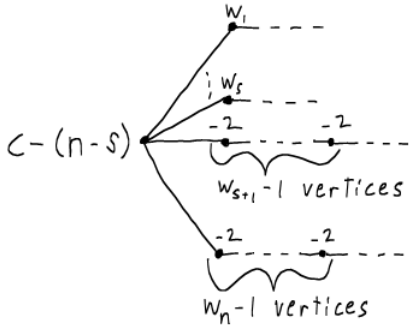

Figure 3.14: Local diagram of (Γ', W') after applying sequence of moves from $\{\text{M1c}, \text{M1c}^{-1}\}$, as prescribed in the algorithm of Theorem 3.1.7

To finish bringing (Γ', W') to normal form requires performing more moves from $\{\text{M1b},\text{M1b}^{-1},\text{M1c},\text{M1c}^{-1}\}$ until no vertex lying in a chain has weight greater than -2. In Figure 3.14 above, no vertex adjacent to the central one weighted $c-(n-s)$ has weight greater than -2, so the weight of this vertex remains unchanged throughout the rest of the process. It follows that after bringing (Γ', W') to normal form, it has local diagram shown in Figure 3.15, for some integers $w_i' \leq -2$.

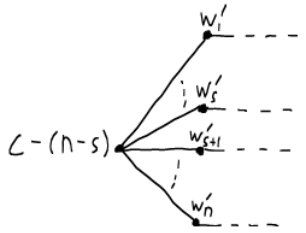

Figure 3.15: Local diagram of (Γ', W') after bringing it to normal form.

So then the local diagram in Figure 3.15 is from a weighted graph in normal form representing the Seifert fibered space with normalized invariants $\{Oo0\big|b;(\alpha_1,\beta_1),\dots(\alpha_n,\beta_n)\}$. But the local diagram in Figure 3.9 is also from a weighted graph in normal form representing the Seifert fibered space with normalized invariants $\{Oo0\big|b;(\alpha_1,\beta_1),\dots(\alpha_n,\beta_n)\}$. Then by uniqueness from Theorem 3.1.8, these local diagrams must be the same. This implies the weights of the central vertices are equal, in other words $-b-n=c-(n-s)$. This implies $c=-b-s$. Substituting this new value for c into the local diagram of (Γ', W') from Figure 3.13, we obtain the local diagram for (Γ', W') shown in Figure 3.16.

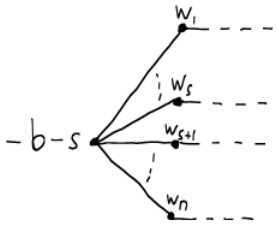

Figure 3.16: Local diagram of (Γ', W'). The central vertex weighted $-b-s$ is referred to as v in the succeeding paragraph.

Using this form of (Γ', W'), we will derive a contradiction.

Since (Γ', W') was obtained from (Γ, W) by a sequence of {M1a,M1b,M1c,M2,M3} (but not their inverses), Theorem 2.0.7 implies (Γ', W') admits an EFe-labeling since (Γ, W) does. From the diagram in Figure 3.16, we see (Γ', W') has a unique vertex v with valence $n \geq 3$, which has weight $-b-s$. Now, any vertex labeled e must have valence equal to 1 by property e2 from Definition 2.0.6, so v cannot be labeled e. So first assume v has label F. Consider any w_i with $i \leq s$. w_i is negative, by our definition of s, so the vertex it weights must have label F or e. The rest of the vertices have weights at least 2, so cannot be labeled F or e. So then there is a total of s vertices to v by an edge having label F or e, or in other words, $\text{eval}(v) + \text{Fval}(v) = s$. But then we have

$$\begin{array}{rcll} W'(v) & = & -b-s & \text{from Figure 3.16} \\ & > & -s & \text{assumption that } b<0 \\ & = & -(\text{eval}(v)+\text{Fval}(v)) & \text{discussion above} \\ & \geq & W'(v) & \text{property F1} \end{array}$$

which is a contradiction.

So the last available option is that the label of v is E. Since the total valence of v is n, $\text{eval}(v) + \text{Eval}(v) + \text{Fval}(v) = n$, and then since $\text{eval}(v) + \text{Fval}(v) = s$, $\text{Eval}(v) = n-s$. Consequently,

$$\begin{array}{rcll} n & = & n-s+s & \\ & = & \text{Eval}(v)+s & \text{preceding discussion} \\ & \leq & W'(v)+s & \text{property E1} \\ & = & -b-s+s & \text{from Figure 3.16} \\ & = & -b & \\ & < & n & \text{assumption that } -n<b \end{array}$$

which is a contradiction. Q.E.D.

Chapter 4

3-Manifolds from Cellulated 2-Disks

In this chapter, we formally define cycle-free twisted face-pairing manifolds in Definition 4.2.1. Some of the main results of this chapter are Theorems 4.1.3 and 4.2.3, which imply that cycle-free twisted face-pairing manifolds can always be plumbed from weighted graphs admitting an EFe-labeling. This can be seen as the source of motivation for studying EFe-labelings.

4.1 Cycle-free Cellulations and Their Weighted Graphs

Definition 4.1.1. In this chapter, a **cellulation of D^2**, or a **cellulation of the 2-disk**, or just a **cellulation**, if it is clear from the context, will mean a CW-complex structure on D^2. A **cycle-free cellulation of D^2**, or often just **cycle-free cellulation**, if clear from the context, is a cellulation of D^2 without any vertices contained in the interior of D^2, $\{(x, y) \in D^2 : x^2 + y^2 < 1\}$, so all the vertices are contained in the boundary circle, $\{(x, y) \in \mathbb{R}^2 : x^2 + y^2 = 1\}$. Note that since D^2 is compact, any cellulation of it will be finite.

Definition 4.1.2. For any cellulation C of D^2 with k_F (closed) faces, $\{F_i\}_{i=1}^{k_F}$, and k_E (closed) edges, $\{E_i\}_{i=1}^{k_E}$, and any set of k_E integers, $S = \{m_i\}_{i=1}^{k_E} \subseteq \mathbb{Z}$, define the weighted graph $(\boldsymbol{\Gamma_C, W_S})$ as the unique weighted graph satisfying the following conditions:

1. There are injective maps $v_F : \{F_i\}_{i=1}^{k_F} \to V(\Gamma_C)$ and $v_E : \{E_i\}_{i=1}^{k_E} \to V(\Gamma_C)$ from the sequences of edges and faces of C to the set of vertices of Γ_C. If $v \in \mathrm{im}\,(v_F)$, we often say that "v corresponds to a face of C". If $v \in \mathrm{im}\,(v_E)$, we often say that "v corresponds to an edge C".

2. If $E_i \subseteq F_j$ for some i, j, then there is an edge of Γ_C connecting $v_E(E_i)$ and $v_F(F_j)$.

3. There is an injective map $v_e : \{E_i\}_{i=1}^{k_E} \to V(\Gamma_C)$ from the sequences of edges of C to the set of vertices of Γ_C. If $v \in \mathrm{im}\,(v_e)$, we often also say that "v corresponds to an edge C".

4. For each edge E_i of C, there is an edge of Γ_C connecting $v_E(E_i)$ and $v_e(E_i)$.

5. $\mathrm{im}\,(v_F)$, $\mathrm{im}\,(v_E)$, and $\mathrm{im}\,(v_e)$ are pairwise disjoint, and $\mathrm{im}\,(v_F) \cup \mathrm{im}\,(v_E) \cup \mathrm{im}\,(v_e) = V(\Gamma_C)$ $((\mathrm{im}\,(v_F), \mathrm{im}\,(v_E), \mathrm{im}\,(v_e))$ partitions $V(\Gamma_C))$. So for every face of C, there is one corresponding vertex of Γ_C, and for every edge of C, there are two corresponding vertices of Γ_C. Each of these vertices are distinct, and these are all the vertices of Γ_C. This uniquely determines the vertices of Γ_C.

6. The number of edges of Γ_C is minimal, subject to conditions 1-5. This uniquely determines the edges of Γ_C.

7. The weight of any vertex in $\mathrm{im}\,(v_F)$ or $\mathrm{im}\,(v_E)$ is 0, and the weight of $v_e(E_i)$, $W_S(v_e(E_i))$, is m_i. By 5, this uniquely defines a weight for each vertex of Γ_C.

The notation Γ_C indicates that the graph only depends on the cellulation C and not the set of integers S, and the notation W_S indicates that the weighting depends on S (and implicitly on the graph). We often say that "Γ_C arises from a cellulation" and "(Γ_C, W_S) arises from a cellulation and a sequence of integers". Examples of cycle-free cellulations C (shown in black) of D^2 and the weighted graphs Γ_C for some sequences of integers S are depicted below in Figure 4.1.

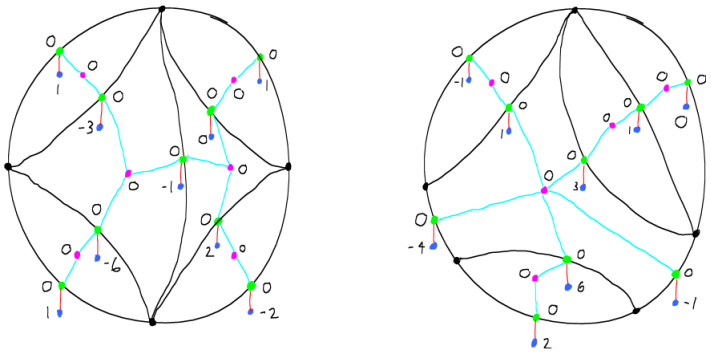

Figure 4.1: Two examples of weighted graphs constructed from cellulated disks. The vertices in $\mathrm{im}\,(v_F)$ are shown in pink, those in $\mathrm{im}\,(v_E)$ are shown in green, and those in $\mathrm{im}\,(v_e)$ are blue. The edges arising from condition 2 are shown in light blue, and those from condition 4 are red. The weights of the vertices in $\mathrm{im}\,(v_e)$ are printed in black near the vertices, and the weights of all other vertices are 0.

Remarks: The above conditions give an axiomatic definition of Γ_C, which is useful for proving theorems, and thus the preferred definition, but may not allow one to immediately visualize the graph. To that end, Γ_C may also be defined in a constructive manner, and the reader may wish to keep this construction in mind. The construction was previously discussed in the remarks following Definition 2.0.6, and we review it here. Firstly, add one vertex to Γ_C for each edge and face of C, and weight these vertices 0. Secondly, add an edge to Γ_C connecting vertices v_1 and v_2 if v_1 corresponds to a face F of C, v_2 corresponds to an edge E of C, and F contains E. Thirdly, adjoin a single edge and vertex to each vertex of Γ_C that corresponds to an edge C, and weight these new vertices with arbitrary integers. Figure 4.2 shows an example of such a construction.

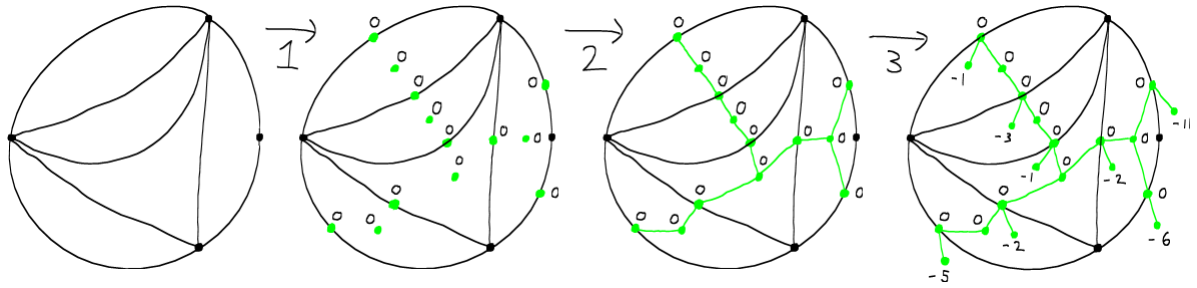

Figure 4.2: Construction of the weighted graph Γ_C from a CW-complex C with underlying space D^2. C is drawn in black and Γ_C in green. The first step adds vertices weighted 0 to Γ_C for each edge and face of C. The second step adds an edge to Γ_C for each pair of vertices $\{v_1, v_2\}$ such that v_1 corresponds to a face F of C, v_2 corresponds to an edge E of C, and F contains E. The edge connects v_1 and v_2. The third step adjoins a single edge and vertex to each vertex of Γ_C that corresponds to an edge C, and weights these new vertices with arbitrary negative integers.

Theorem 4.1.3. Let (Γ, W) be a weighted graph. If $(\Gamma, W) = (\Gamma_C, W_S)$ for some cycle-free cellulation C of D^2 and sequence of *negative* integers S, then (Γ, W) admits an EFe-labeling.

Proof. Assume $(\Gamma, W) = (\Gamma_C, W_S)$ for some cycle-free cellulation C of D^2 and sequence of negative integers S. We will define a labeling L such that (Γ, W, L) is an EFe-labeled graph. By conditions 1 and 3 of Definition 4.1.2, there exist an injective map v_F from the faces of C to the vertices of Γ and injective maps v_E and v_e from the edges of C to the vertices of Γ. For any $v \in V(\Gamma)$, let $L(v) = F$ if $v \in \mathrm{im}\,(v_F)$, $L(v) = E$ if $v \in \mathrm{im}\,(v_E)$, and $L(v) = e$ if $v \in \mathrm{im}\,(v_e)$. This is a well-definition of L since by condition 5, $(\mathrm{im}\,(v_F), \mathrm{im}\,(v_E), \mathrm{im}\,(v_e))$ partition Γ. It remains to show L satisfies the defining properties of an EFe-labeling from Definition 2.0.6.

Consider any vertex v of Γ labeled E. Then $v = v_E(E_i)$ for some edge E_i of C. Since C is a cellulation of D^2, then E_i is contained in exactly one or two faces of C. First assume there are

two such faces, and call one F_{i_1} and the other F_{i_2}. By conditions 1 and 2 of Definition 4.1.2, $v_F(F_{i_1})$ and $v_F(F_{i_2})$ are distinct vertices of Γ, and there is an edge connecting v to $v_F(F_{i_1})$ and an edge connecting v to $v_F(F_{i_2})$. Let $v_1 = v_F(F_{i_1})$ and $v_2 = v_F(F_{i_2})$. By conditions 4 and 5, $v_e(E_i)$ is a vertex of Γ distinct from $v_F(F_{i_1})$ and $v_F(F_{i_2})$, and connected to $v = v_E(E_i)$ by an edge. Let $v_3 = v_e(E_i)$. By condition 6, these are all the edges containing v. Now, by definition of L, $L(v_1) = L(v_2) = \mathrm{F}$ and $L(v_3) = \mathrm{e}$. So in summary we have $W(v) = 0$ (by condition 7), $L(v) = \mathrm{E}$, $\mathrm{Eval}(v) = 0$, $\mathrm{Fval}(v) = 2$, and $\mathrm{eval}(v) = 1$. Then

$$W(v) = 0 \geq 0 = \mathrm{Eval}(v)$$

$$\mathrm{Eval}(v) + \mathrm{Fval}(v) = 0 + 2 \leq 2$$

and so v satisfies the two properties of an E-labeled vertex. The case where E_i is contained in only one face can be checked similarly.

Next, consider a vertex v of Γ labeled F. Then $v = v_F(F_i)$ for some face F_i of C. Let $\{E_{i_j}\}_{j=1}^{k_{F_i}}$ be the sequence of edges that are contained in F_i. By condition 1 of Definition 4.1.2, $v_E(\{E_{i_j}\}_{j=1}^{k_{F_i}})$ is a set of k_{F_i} distinct vertices of Γ. By conditions 2 and 6, for each j, there is exactly one edge connecting $v_E(E_{i_j})$ to v, and these are all the edges containing v. Now, by definition of L, $L(v_E(E_{i_j})) = \mathrm{E}$. So in summary, we have $W(v) = 0$ (by condition 7), $L(v) = \mathrm{F}$, $\mathrm{Eval}(v) = k_{F_i}$, $\mathrm{Fval}(v) = 0$, and $\mathrm{eval}(v) = 0$. Then

$$W(v) = 0 \leq 0 = -(0 + 0) = -(\mathrm{Fval}(v) + \mathrm{eval}(v))$$

and so v satisfies the one property of an F-labeled vertex.

Finally, consider a vertex v of Γ labeled e. Then $v = v_e(E_i)$ for some edge E_i of C. By conditions 4 and 6 of Definition 4.1.2, there is an edge of Γ connecting v to $v_E(E_i)$, and this is the only edge containing v. Now, by definition of L, $L(v_E(E_i)) = \mathrm{E}$. So in summary, we have $W(v) = -m_i$ (by condition 7, where $m_i \in \mathbb{Z}_{>0}$, since S has only negative integers), $L(v) = \mathrm{e}$, $\mathrm{Eval}(v) = 1$, $\mathrm{Fval}(v) = 0$, and $\mathrm{eval}(v) = 0$. Then

$$W(v) = -m_i \leq -1 = -(1 + 0) = -(1 + \mathrm{Fval}(v))$$

$$\mathrm{val}(v) = \mathrm{Eval}(v) + \mathrm{Fval}(v) + \mathrm{eval}(v) = 1 + 0 + 0 = 1$$

$$\mathrm{eval}(v) = 0$$

and so v satisfies the three properties of an e-labeled vertex. Q.E.D.

Remarks: In the remarks following Definition 4.1.2, we introduced a three-step procedure to construct the weighted graph Γ_C from a cycle-free cellulation C. The proof of Theorem

4.1.3 prescribes an EFe-labeling of Γ_C. With this construction of Γ_C in mind, we summarize said EFe-labeling: The vertices added to Γ_C in the first step that correspond to edges of C are labeled E. The vertices added to Γ_C in the first step that correspond to faces of C are labeled F. The vertices added to Γ_C in the third step are labeled e. This is the origin for the 'EFe' prefix in 'EFe-labeling'. The EFe-labeling for the example in Figure 4.2 is shown in the diagram in Figure 4.3.

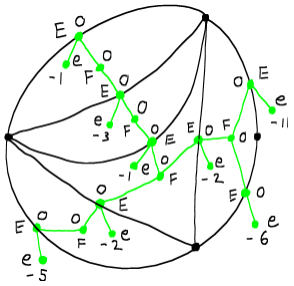

Figure 4.3: EFe-labeling of the weighted graph Γ_C constructed from the cycle-free cellulation C. C is drawn in black and Γ_C in green.

Theorem 4.1.4. Let (Γ, W) be a weighted graph. If $(\Gamma, W) = (\Gamma_C, W_S)$ for some cycle-free cellulation C of D^2 and sequence of integers S, then Γ is a tree, i.e., Γ is connected and cycle-free. We also mention, but do not prove, that if C were to have interior vertices, then Γ_C will have cycles. This is the origin of the 'cycle-free' prefix in 'cycle-free cellulation'.

Proof. The proof is by induction on k_E, the number of edges of C. For the base case, suppose C has exactly 1 edge. Then C must be the standard minimal CW-complex structure on D^2, with exactly 1 face, 1 edge, and 1 vertex. Then in this case, Γ_C will consist of 3 vertices connected by 2 edges, and so Γ_C is a tree. A diagram of this cellulation and corresponding graph is shown in Figure 4.4.

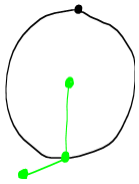

Figure 4.4: Graph associated to a cycle-free cellulation with exactly 1 edge. The cellulation is shown in black and the graph is green. The graph is a tree.

Now assume that, for some $k_E > 1$, if C is a cycle-free cellulation of D^2 with $k_E - 1$ edges, then Γ_C is a tree. Let C be a cycle-free cellulation of D^2 with k_E edges. Let v_F, v_E, and v_e be maps for Γ_C as in Definition 4.1.2. We will treat two cases: C has no interior edges

(edges not contained in the boundary circle of D^2), and C has at least one interior edge (an edge that intersects the interior of D^2).

In the first case, C has exactly 1 face, k_E edges and k_E vertices. Let F be the face and E_i one of the edges. By conditions 1 and 2 from Definition 4.1.2, there is a vertex $v_1 = v_F(F)$ of Γ_C corresponding to F and a vertex $v_2 = v_E(E_i)$ corresponding to E_i and an edge connecting them. By conditions 3, 4, and 5, there is another vertex $v_3 = v_e(E_i)$ corresponding to E_i, and it is connected to v_2 by an edge. Since F is the only face containing E_i, then by condition 6, these two edges mentioned are the only edges of Γ_C containing v_2 and v_3. A local diagram of C near E_i and the corresponding local diagram of Γ_C is shown on the left in Figure 4.5. Note that the diagram must be of this form since there are at least 2 edges and they are all contained in the boundary circle. Now consider the cycle-free cellulation C' of D^2 obtained by collapsing E_i to a single vertex. Then C' will have exactly 1 face, $k_E - 1$ edges, and $k_E - 1$ vertices. So since there is now 1 less edge, the corresponding graph $\Gamma_{C'}$ will be identical to Γ_C except that the vertices and edges corresponding to E_i will be deleted. A local diagram of C' and $\Gamma_{C'}$ is shown on the right in Figure 4.5.

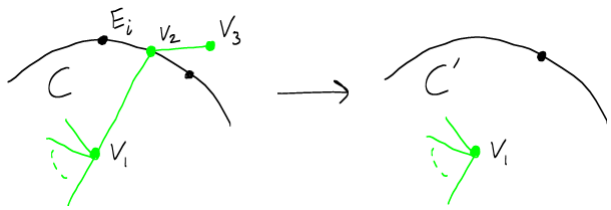

Figure 4.5: Local diagrams of C and the corresponding graph Γ_C shown on left, and local diagrams of C' and the corresponding graph $\Gamma_{C'}$ shown on right. C' is obtained from C by collapsing an edge to a single vertex, which results in deleting 2 edges and 2 vertices from the graph.

It is clear from the diagram that $\Gamma_{C'}$ is obtained from Γ_C by a local transformation, and that this transformation can neither connect the graph, disconnect the graph, introduction a cycle, nor remove a cycle. So Γ_C is a tree if and only if $\Gamma_{C'}$ is a tree. Since C' has $k_E - 1$ edges, $\Gamma_{C'}$ is a tree by the inductive hypothesis, so Γ_C is also.

Now we consider the case in which there exists an interior edge E_j of C. There are two situations that can occur: E_j contains exactly 1 vertex, which lies on the boundary circle of D^2, and E_j contains exactly 2 vertices, which both lie on the boundary circle of D^2. These two situations are shown in Figure 4.6.

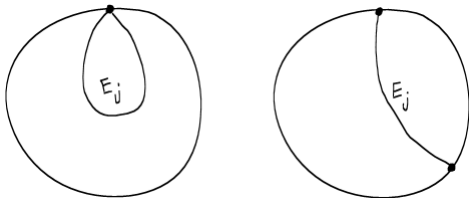

Figure 4.6: The two possibilities for edge E_j which intersects the interior of D^2.

In either case, E_j is contained in exactly 2 faces of C, as a consequence of the Jordan curve theorem. Note that this would not necessarily be the case if E_j contained a vertex in the interior of D^2. Let F_1 and F_2 be the two faces containing E_j. By conditions 1 and 2 from Definition 4.1.2, there is a vertex $v_1 = v_F(F_1)$ of Γ_C corresponding to F_1, a vertex $v_2 = v_F(F_2)$ of Γ_C corresponding to F_2, a vertex $v_3 = v_E(E_j)$ of Γ_C corresponding to E_j, and edges connecting v_1 to v_3 and v_2 to v_3. By conditions 3, 4, and 5, there is another vertex $v_4 = v_e(E_j)$ corresponding to E_i, and it is connected to v_3 by an edge. Since F_1 and F_2 are the only faces containing E_j, then by condition 6, these three edges mentioned are the only edges of Γ_C containing v_3 and v_4. A local diagram of C near E_j and the corresponding local diagram of Γ_C is shown on the left in Figure 4.8. Now consider the cycle-free cellulation C' of D^2 obtained by removing the edge E_j and replacing the faces F_1 and F_2 with the single face $F' = F_1 \cup F_2$. Two examples of such cellulations C and C' are shown in Figure 4.7. Then C' will have one less face and one less edge than C and the same number of vertices. The corresponding graph $\Gamma_{C'}$ is obtained from C by deleting the vertices v_3 and v_4 and the edges that contained them, and merging the vertices v_1 and v_2 into a single vertex v'. C' and a local diagram of $\Gamma_{C'}$ is shown in Figure 4.8.

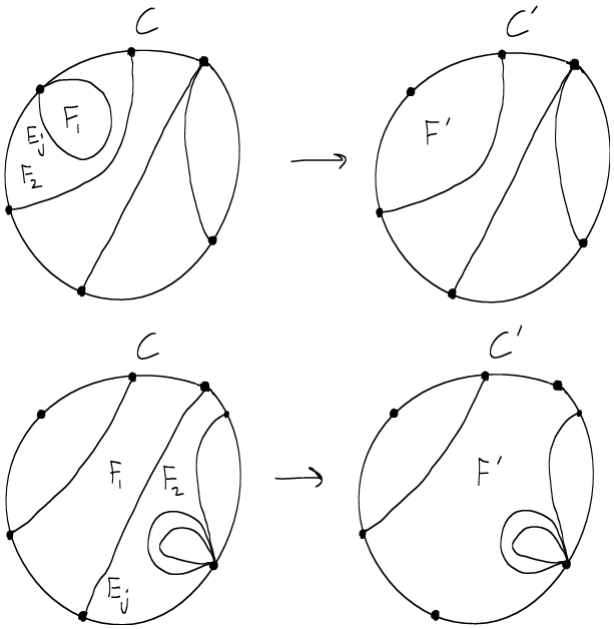

Figure 4.7: Diagrams of two examples of cycle-free cellulations C and C'. C' is obtained from C by deleting E_j and replacing F_1 and F_2 with $F' = F_1 \cup F_2$.

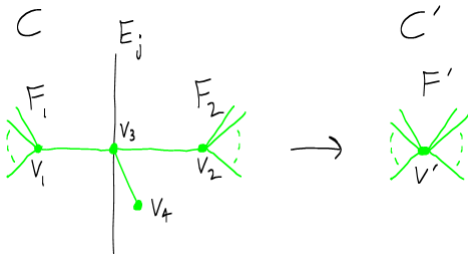

Figure 4.8: Local diagrams of C and corresponding graph Γ_C shown on left, and local diagrams of C' and corresponding graph $\Gamma_{C'}$ shown on right. C' is obtained from C by deleting an edge and joining the two faces that contained it, which results in deleting 3 edges and 2 vertices from the graph and merging two vertices into one.

It can be seen from Figure 4.8 that $\Gamma_{C'}$ is obtained from Γ_C by a local move that neither connects the graph, disconnects the graph, introduces a cycle, nor removes a cycle. Then Γ_C is a tree if and only if $\Gamma_{C'}$ is a tree. Since C' has $k_E - 1$ edges, $\Gamma_{C'}$ is a tree by the inductive hypothesis. Thus, Γ_C is a tree. This exhausts all the cases and proves the theorem. Q.E.D.

4.2 Cycle-Free Twisted Face-Pairing Manifolds

Definition 4.2.1. Let C be a cycle-free cellulation of D^2. Let ϕ_N and ϕ_S be the natural projection homeomorphisms from the northern hemisphere of S^2, $\{(x, y, z) \in S^2 : z \geq 0\}$, and southern hemisphere of S^2, $\{(x, y, z) \in S^2 : z \leq 0\}$, respectively, to D^2. Then C pulls back to CW-complex structures C_N and C_S of the northern and southern hemispheres of S^2 under ϕ_N and ϕ_S. For each face $F_i \in \{F_i\}_{i=1}^{k_F}$ of C_N, let $\epsilon_i = (\phi_S^{-1} \circ \phi_N)\big|_{F_i}$. Then the **cycle-free reflection face-pairing constructed from C**, denoted $\boldsymbol{\epsilon_C}$, is the collection $\{\epsilon_i\}_{i=1}^{k_F}$, which forms a reflection face-pairing on the faceted 3-ball $C_S \cup C_N \cup \mathring{D}^3$. Reflection face-pairings are defined in Section 3 of [4].

Definition 4.2.2. Let C be a cycle-free cellulation of D^2 and ϵ_C its associated cycle-free reflection face-pairing. Let *mult* be a multiplier function for ϵ_C, which is a sequence of positive integers corresponding to the edge cycles of ϵ_C. Let $\boldsymbol{M(\epsilon_C, mult)}$ be the associated oriented twisted face-pairing manifold, defined in Section 2 of [1]. Then $M(\epsilon_C, mult)$ is called a **cycle-free twisted face-pairing manifold**. The 'reflection face-pairing' name comes from the fact that ϵ_C is a reflection face-pairing in the sense of [4], and the 'cycle-free' prefix comes from the fact that C has no interior vertices, so by Theorem 4.1.4, its associated weighted graph Γ_C is cycle-free in the graph-theoretic sense. Any 3-manifold homeomorphic to $M(\epsilon_C, mult)$ for some cycle-free cellulation C of D^2 and some multiplier function *mult* is also called a cycle-free twisted face-pairing manifold.

Theorem 4.2.3. If C is a cellulation of D^2 and $S = \{-m_i\}$ is a sequence of negative integers equal to the negative of a multiplier function $mult = \{m_i\}$ for the edge cycles of the reflection face-pairing ϵ_C, then the twisted face-pairing manifold $M(\epsilon, mult)$ is orientation-preservingly homeomorphic to the 3-manifold $N(\Gamma_C, W_S)$ obtained by plumbing on (Γ_C, W_S).

Proof. Let C be a cellulation of D^2. Let $\{F_i\}_{i=1}^{k_F}$ and $\{E_i\}_{i=1}^{k_E}$ be the sequence of faces and set of edges, respectively, of C. Let ϵ be the reflection face-pairing associated with C. Let $mult = \{m_i\}_{i=1}^{k_E}$ be the multiplier function for the set of edge cycles of ϵ. Let $S = \{-m_i\}_{i=1}^{k_E}$. First, we will define a framed link L in S^3 constructed from (Γ_C, W_S). For every vertex v of Γ_C, there is an unknotted component of L with framing $W(v)$. If v_1 and v_2 are vertices of Γ_C connected by an edge, then their corresponding components are linked once in L. If v_1 and v_2 are not connected by an edge, then their corresponding components in L are unlinked. Since Γ is a tree from the previous theorem, these conditions uniquely determine L up to isotopy. In particular, we did not need to consider orientations when specifying the linking of components. It follows from the discussion preceding Figure 1.6 on page 13 of [10] that the manifold resulting from Dehn surgery on L is orientation-preservingly homeomorphic to $N(\Gamma_C, W_S)$. An example of a weighted tree and the corresponding link is shown below in Figure 4.9.

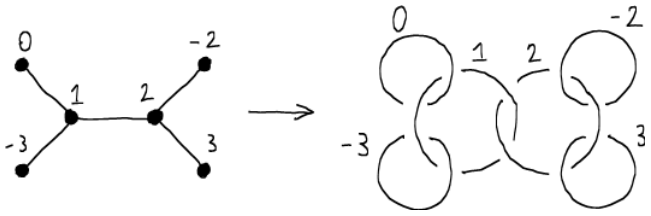

Figure 4.9: The framed link corresponding to a plumbing graph.

Next, we will transform L to a framed link L' via the Kirby calculus, so that Dehn surgery on L' will yield a manifold orientation-preservingly homeomorphic to that obtained by surgery on L, and hence orientation-preservingly homeomorphic to $N(\Gamma_C, W_S)$.

Now, by condition 3 of Definition 4.1.2, there exists an injective map v_e from the edges of C to the vertices of Γ_C satisfying $W_S(v_e(E_i)) = -m_i$ for each i by condition 7. Furthermore, by condition 1, there exist injective maps v_F and v_E from the edges and faces of C, respectively, to the vertices of Γ_C. For each i, by conditions 4 and 6, there is an edge connecting $v_e(E_i)$ and $v_E(E_i)$, and this is the only edge containing $v_e(E_i)$. By condition 7, $W_S(v_E(E_i)) = 0$. A local diagram of Γ_C containing such a vertex is shown below in Figure 4.10, as well as the corresponding local diagram of L.

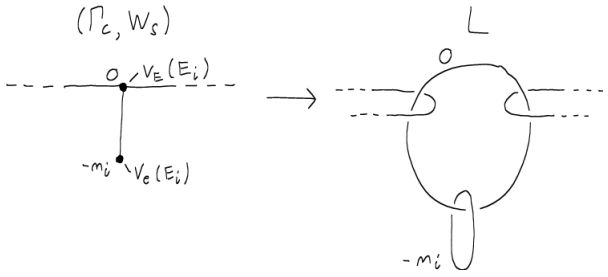

Figure 4.10: Local diagram of Γ_C containing the vertex $v_e(E_i)$, and the local diagram of the corresponding framed link.

By performing a slam-dunk move on each of these components framed $-m_i$, we obtain the new link L'. Local diagrams of L and L' containing the components involved in the slam-dunk are shown below in Figure 4.11.

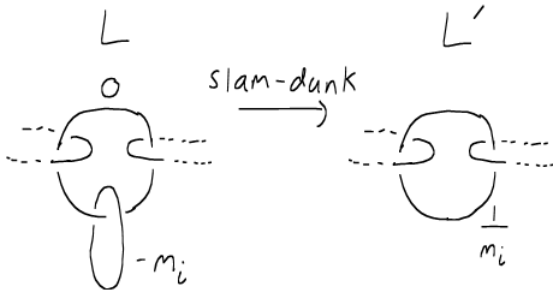

Figure 4.11: Transforming the framed link L to L' under the slam-dunk move. Performing Dehn surgery on L yields a manifold homeomorphic to that obtained by Dehn surgery on L'.

An overall summary of this process going from (Γ_C, W_S) to L to L' using an example cellulation C and set of negative integers S is shown in Figure 4.12.

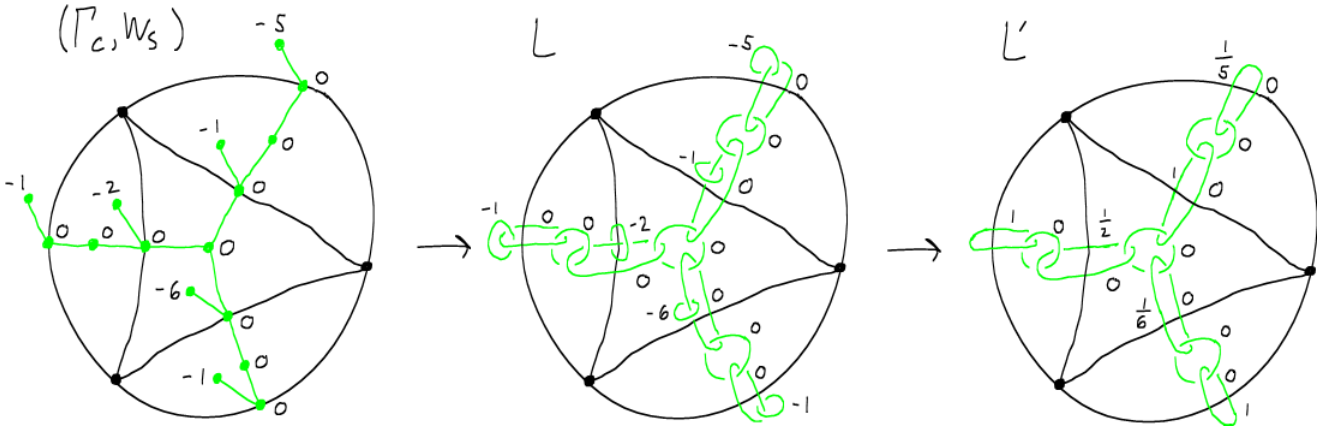

Figure 4.12: Summary of the process of taking (Γ_C, W_S) to L to L' (all drawn in green) for an example cellulation C (drawn in black) and an example set of negative integers S.

The link L' now satisfies the following properties:

1. There is a bijective correspondence between the set of edges and faces of C, $\{E_i\}_{i=1}^{k_E} \cup \{F_i\}_{i=1}^{k_F}$, to the components of L', denoted $E_i \mapsto J_{E_i}$ or $F_i \mapsto J_{F_i}$.
2. J_{E_i} and J_{F_i} are unknotted for all E_i and F_i.
3. If E_i is an edge of C contained in a face F_i of C, then J_{F_i} and J_{E_i} link once in L'.
4. If E_i is an edge of C not contained in a face F_i of C, then J_{F_i} and J_{E_i} do not link in L'.

5. The framing of J_{E_i} is $\frac{1}{m_i}$, and the framing of J_{F_i} is 0 for all i.

It follows from Theorem 3.2 from [4] that Dehn surgery on L' yields a manifold orientation-preservingly homeomorphic to $M(\epsilon, mult)$. Q.E.D.

Chapter 5

Cycle-Free Twisted Face-Pairing Manifolds and Seifert Fibered Spaces

We conclude this paper with a classification of the Seifert fibered spaces over S^2 that are cycle-free twisted face-pairing manifolds. This is the content of Theorem 5.1.5, the main result of this chapter, and of the entire paper. We also apply this result to classify the spherical space forms that are cycle-free twisted face-pairing manifolds.

5.1 Seifert Fibered Spaces over S^2

Theorem 5.1.1. If M is an oriented Seifert fibered space over S^2 with normalized invariants $\{Oo0\big|b; (\alpha_1, \beta_1), \ldots (\alpha_n, \beta_n)\}$ such that $n \geq 3$ and $-n < b < 0$, then M is not orientation-preservingly homeomorphic to $M(\epsilon_C, mult)$ for any cycle-free cellulation C of D^2 and multiplier function $mult$, i.e., M is not a cycle-free twisted face-pairing manifold.

Proof. We will prove the contrapositive. Let M be an oriented 3-manifold orientation-preservingly homeomorphic to $M(\epsilon_C, mult)$ for some cycle-free cellulation C of D^2 and multiplier function $mult$. Let $S = \{-m_i\}$ where $mult = \{m_i\}$. Then by Theorem 4.2.3, M is orientation-preservingly homeomorphic to $N(\Gamma_C, W_S)$. By Theorem 4.1.3, (Γ_C, W_S) admits an EFe-labeling. But then by Theorem 3.2.3, $N(\Gamma_C, W_S)$ is not orientation-preservingly homeomorphic to any oriented Seifert fibered space over S^2 with normalized invariants $\{Oo0\big|b; (\alpha_1, \beta_1), \ldots (\alpha_n, \beta_n)\}$ such that $n \geq 3$ and $-n < b < 0$. Q.E.D.

We will next prove a partial converse to Theorem 5.1.1. By this, we mean that we wish to construct cycle-free cellulations C of D^2 and multiplier functions $mult$ so that $M(\epsilon_C, mult)$

is a Seifert fibered space with normalized invariants not of the form in Theorem 5.1.1. We will be able to achieve this in many cases, and this is the content of Theorem 5.1.4. We will first prove two preliminary results, Lemmas 5.1.2 and 5.1.3. Lemma 5.1.3 is the main ingredient in the proof of Theorem 5.1.4. It is a useful tool which gives us a controlled way to combine weighted graphs arising from cycle-free cellulations into new weighted graphs that also arise from cycle-free cellulations.

Lemma 5.1.2 is a result about combining two cycle-free cellulations into a new cycle-free cellulation. An example of such a combination is shown in Figure 5.1, and the reader should keep this example in mind while reading the statement of Lemma 5.1.2. This diagram is shown again in Figure 5.3 in the middle of the proof of Lemma 5.1.2.

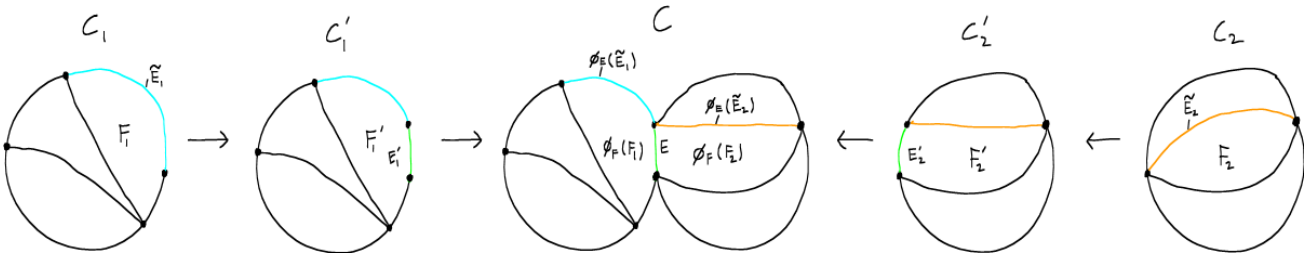

Figure 5.1: Construction of C from the example cellulations C_1 and C_2, as in Lemma 5.1.2. This diagram is shown again in Figure 5.3.

Lemma 5.1.2. Let C_1 and C_2 be cycle-free cellulations of D^2, with sequences of edges and faces $\{E_1^j\}_{j=1}^{k_1^E}$, $\{E_2^j\}_{j=1}^{k_2^E}$, $\{F_1^j\}_{j=1}^{k_1^F}$, and $\{F_2^j\}_{j=1}^{k_2^F}$. Then for any pair of faces $F_1 \subseteq C_1$ and $F_2 \subseteq C_2$, there exists a cycle-free cellulation C of D^2, having sequences of edges $\{E^j\}_{j=1}^{k^E}$ and faces $\{F^j\}_{j=1}^{k^F}$, and there exist maps $\phi_E : \{E_1^j\}_{j=1}^{k_1^E} \sqcup \{E_2^j\}_{j=1}^{k_2^E} \to \{E^j\}_{j=1}^{k^E}$ and $\phi_F : \{F_1^j\}_{j=1}^{k_1^F} \sqcup \{F_2^j\}_{j=1}^{k_2^E} \to \{F^j\}_{j=1}^{k^F}$ satisfying the following conditions:

1. If E^j is an edge of $C_1 \sqcup C_2$ contained in a face F^j of $C_1 \sqcup C_2$, then $\phi_E(E^j)$ is contained in $\phi_F(F^j)$.
2. ϕ_F is bijective.
3. ϕ_E is injective.
4. There is an edge E of C such that
   (a) ϕ_E is not surjective, but $\{E^j\}_{j=1}^{k^E} = \mathrm{im}\,(\phi_E) \cup \{E\}$ (so ϕ_E misses 1 edge).
   (b) E is contained in the faces $\phi_F(F_1)$, $\phi_F(F_2)$ of C (since C is cycle-free, it follows that $E = \phi_F(F_1) \cap \phi_F(F_2)$).

Proof. Let F_1, F_2 be as in the statement of the lemma. We locally modify C_i near F_i to obtain a new cycle-free cellulation C_i' of D^2 by replacing any vertex contained in F_i by an edge E_i'. This process is shown in Figure 5.2 for four example situations.

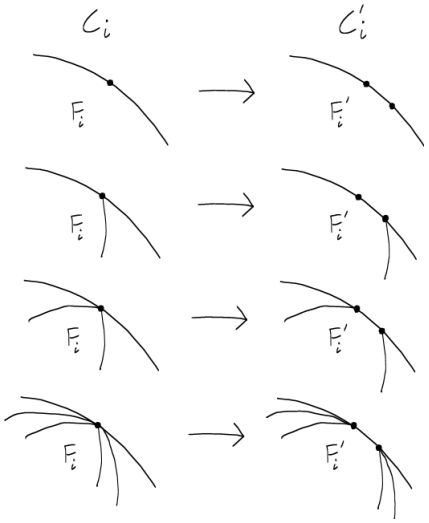

Figure 5.2: Modifying a cycle-free cellulation by inserting an edge.

This is very similar to the technique referred to as "splitting edges" by Cannon, Floyd, and Parry in the proof of Theorem 6.1 from [4].

We then define C to be the CW-complex resulting from gluing C_1' and C_2' together by a homeomorphism between E_1' and E_2'. C then has underlying space homeomorphic to D^2, and all its vertices are contained on the boundary circle, so we also refer to C as a cycle-free cellulation of D^2. Now, any edge or face of $C_1 \sqcup C_2$ has a natural image in $C_1' \sqcup C_2'$ which is again an edge or face, and any edge or face in $C_1' \sqcup C_2'$ has a natural image in C which is again an edge of face. We define ϕ_E and ϕ_F to be the composition of those maps just described. We also define E to be the image of E_1' or E_2' in C (it doesn't matter which as these two edges are identified in C). Then C, ϕ_E, ϕ_F, and E satisfy the conditions in the statement of the lemma, as we will now explain. This process is illustrated in Figure 5.3 for example cellulations C_1 and C_2, and the reader should keep this example in mind while reading the explanation.

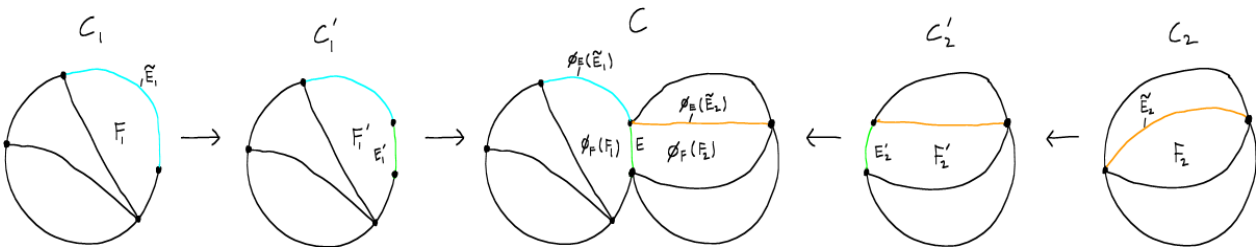

Figure 5.3: Construction of C from the example cellulations C_1 and C_2. Two edges in $C_1 \sqcup C_2$ are highlighted. One called $\tilde{E}_1$ is in blue and the other, $\tilde{E}_2$, is in orange. Their images in $C_1' \sqcup C_2'$ and C have the same coloring. Their images in C are $\phi_E(\tilde{E}_1)$ and $\phi_E(\tilde{E}_2)$, by definition of the map ϕ_E. The inserted edges E_1' and E_2' are colored green, as is their common image E in C. The faces F_1 and F_2 are also labeled, as are their images $\phi_F(F_1)$ and $\phi_F(F_2)$ in C.

1. Condition 1 holds since inserting an edge respects the relationship of containment between edges and faces, as does the quotient map from one complex to another by edge identification, and ϕ_E and ϕ_F result from composing these maps.

2. Condition 2 holds since inserting an edge does not create or destroy any faces, nor does identifying two edges, so we end up with the same number of faces as we started.

3. To see condition 3 holds, first notice that inserting an edge does not delete any edges, so the first map in the composition defining ϕ_E is injective on edges. The second map in the composition defining ϕ_E is the identification of two edges, which is not injective in general. However, the two edges being identified are E_1' and E_2', which are the inserted edges, and thus not in the image of the first map. So the overall composition ϕ_E is injective from edges to edges.

4. Condition 4(a) holds since first 2 new edges are added in the inserting stage, and then 1 edge is removed in the identification stage. This new edge is precisely E. Condition 4(b) holds since E was designed to belong to both F_1 and F_2.

Q.E.D.

We next prove another lemma building off Lemma 5.1.2 which gives a way to combine two weighted graphs arising from cycle-free cellulations into a new weighted graph arising from a cycle-free cellulation. An example of such a combination is shown in Figure 5.4, and the reader should keep this example in mind while reading the statement of Lemma 5.1.3. This diagram is shown again in Figure 5.5 in the middle of the proof of Lemma 5.1.3.

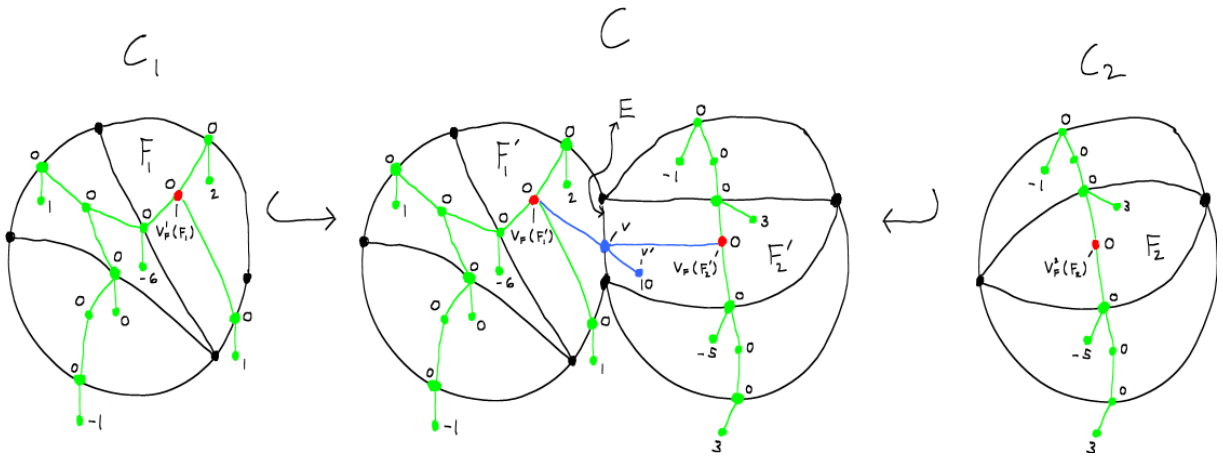

Figure 5.4: The weighted graph Γ_C which is a combination of Γ_{C_1} and Γ_{C_2} (both in green) for the example cellulations C_1 and C_2, as in Lemma 5.1.3. This diagram is shown again in Figure 5.5.

Lemma 5.1.3. Let C_1 and C_2 be cycle-free cellulations of D^2 and $S_1 = \{m_1^j\}_{j=1}^{k_1^E}$, $S_2 = \{m_2^j\}_{j=1}^{k_2^E}$ sequences of integers (superscripts on integers are indices not exponents), where k_i^E is the total number of edges of C_i. Let z be an arbitrary integer, and $S = \{m^j\}_{j=1}^{k_1^E+k_2^E+1}$ the sequence of integers gotten by concatenating S_1, S_2, and $\{z\}$, in that order (so $S = (m^1, \dots m^{k_1^E}, m^{k_1^E+1}, \dots m^{k_1^E+k_2^E}, m^{k_1^E+k_2^E+1}) = (m_1^1, \dots m_1^{k_1^E}, m_2^1, \dots m_2^{k_2^E}, z)$. Let v_F^1, v_E^1, and v_e^1 be the maps for (Γ_{C_1}, W_{S_1}), as in Definition 4.1.2. Likewise for (Γ_{C_2}, W_{S_2}). Then for any pair of faces $F_1 \subseteq C_1$ and $F_2 \subseteq C_2$, there is a cycle-free cellulation C of D^2 such that (Γ_C, W_S) is the unique connected weighted tree satisfying the following conditions:

1. There exists a weighted graph embedding $\iota : (\Gamma_{C_1}, W_{S_1}) \sqcup (\Gamma_{C_2}, W_{S_2}) \to (\Gamma_C, W_S)$ (we will think of ι as an injective map between vertices that preserves edges and weights). So (Γ_{C_1}, W_{S_1}) and (Γ_{C_2}, W_{S_2}) can be identified as weighted subgraphs of (Γ_C, W_S).

   Let v_F, v_E, and v_e be the maps as in Definition 4.1.2 for (Γ_C, W_S).

2. For any face $F_i^j \subseteq C_i$, there is a face $F^j \subseteq C$ such that $v_F(F^j) = \iota(v_F^i(F_i^j))$.

3. There exist 2 vertices $v, v' \in V(\Gamma_C)$ such that

   (a) v and v' and not contained in $\mathrm{im}\,(\iota)$, but $V(\Gamma_C) = \mathrm{im}\,(\iota) \cup \{v, v'\}$

   (b) there is an edge of Γ_C connecting v and $\iota(v_F^1(F_1))$. There is an edge of Γ_C connecting v and $\iota(v_F^2(F_2))$. There is an edge of Γ_C connecting v and v'.

   (c) $W_S(v) = 0$ and $W_S(v') = z$.

Proof. Let C_1 and C_2 be cycle-free cellulations of D^2 with sequences of edges and faces $\{E_1^j\}_{j=1}^{k_1^E}$, $\{E_2^j\}_{j=1}^{k_2^E}$, $\{F_1^j\}_{j=1}^{k_1^F}$, and $\{F_2^j\}_{j=1}^{k_2^F}$. Let $F_1 \subseteq C_1$ and $F_2 \subseteq C_2$ be an arbitrary pair of faces. Let C, ϕ_E, ϕ_F be as in the conclusion of Lemma 5.1.2 with respect to F_1 and F_2. Let E be the edge of C as in condition 4 of the conclusion of Lemma 5.1.2. Then by conditions 3 and 4(a), ϕ_E is injective and fails to be surjective only because it misses E, so we can and do write the sequence of edges of C as the concatenation of $\{\phi_E(E_1^j)\}_{j=1}^{k_1^E}$, $\{\phi_E(E_2^j)\}_{j=1}^{k_2^E}$, and $\{E\}$, in that order. Let v_F, v_E, and v_e be the maps as in Definition 4.1.2 for (Γ_C, W_S).

Define $\iota : V(\Gamma_{C_1}) \sqcup V(\Gamma_{C_2}) \to V(\Gamma_C)$ by:

- $\iota(v) = v_F(\phi_F(F_1^j))$ if $v = v_F^1(F_1^j)$ for some face $F_1^j \subseteq C_1$
- $\iota(v) = v_E(\phi_E(E_1^j))$ if $v = v_E^1(E_1^j)$ for some edge $E_1^j \subseteq C_1$
- $\iota(v) = v_e(\phi_E(E_1^j))$ if $v = v_e^1(E_1^j)$ for some edge $E_1^j \subseteq C_1$
- $\iota(v) = v_F(\phi_F(F_2^j))$ if $v = v_F^2(F_2^j)$ for some face $F_2^j \subseteq C_2$
- $\iota(v) = v_E(\phi_E(E_2^j))$ if $v = v_E^2(E_2^j)$ for some edge $E_2^j \subseteq C_2$
- $\iota(v) = v_e(\phi_E(E_2^j))$ if $v = v_e^2(E_2^j)$ for some edge $E_2^j \subseteq C_2$

ι is well-defined and injective since $(\mathrm{im}\,(v_F^i), \mathrm{im}\,(v_E^i), \mathrm{im}\,(v_e^i))$ partitions Γ_{C_i} by condition 5 from Definition 4.1.2, v_F^i, v_E^i, and v_e^i are all injective by conditions 1 and 3 from Definition 4.1.2, and ϕ_F and ϕ_E are injective by conditions 2 and 3 from Lemma 5.1.2.

Let $v = v_E(E)$ and $v' = v_e(E)$. Then (Γ_C, W_S), ι, v, and v' satisfy the conditions in the statement of the lemma, as we will now explain. We again use the example of Figure 5.3, but this time include the induced weighted graphs in Figure 5.5, and the reader should keep this example in mind while reading the explanation.

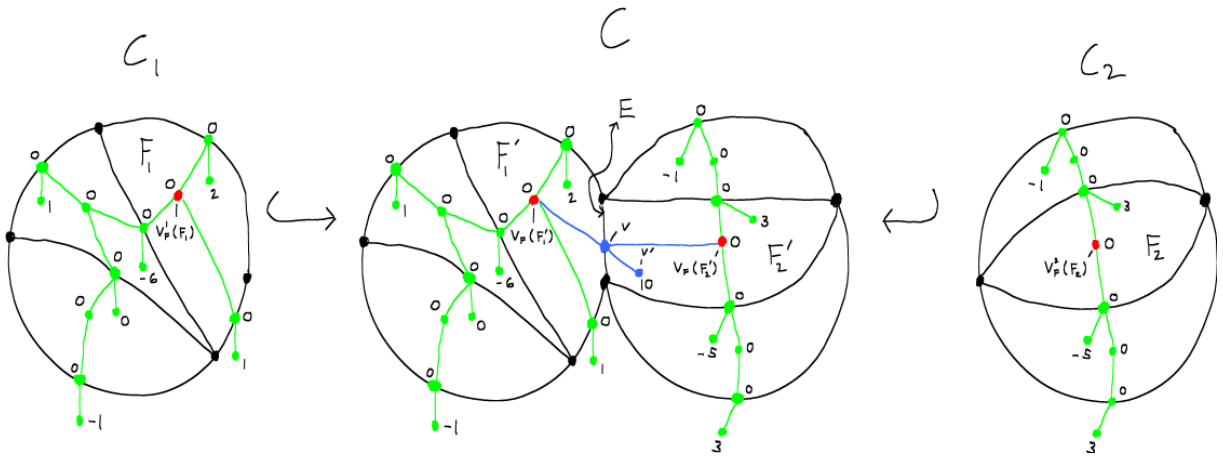

Figure 5.5: The weighted graph Γ_C which contains Γ_{C_1} and Γ_{C_2} as disjoint embedding weighted subgraphs, for the example cellulations C_1 and C_2, sequence of integers S_1 and S_2, and integer $z = 10$. The subgraphs and their embedded images under ι are shown in green. The 2 new vertices v and v' are labeled and colored blue, and the 3 new edges are also blue. The edge E in C is labeled. The faces $F_1 \subseteq C_1$ and $F_2 \subseteq C_2$ and corresponding faces $\phi_F(F_1) = F_1', \phi_F(F_2) = F_2' \subseteq C$ are labeled. Vertices $\iota(v_F^1(F_1)) = v_F(F_1')$ and $\iota(v_F^2(F_2)) = v_F(F_2')$ are labeled and colored red.

1. To show condition 1 of the lemma holds, it remains to show ι respects edges and weights. Suppose v_1 and v_2 are connected by an edge in $\Gamma_{C_1} \sqcup \Gamma_{C_2}$. Then $v_1, v_2 \in V(\Gamma_{C_i})$ for some $i \in \{1, 2\}$. Now, there are three cases: $v_1 = v_F^i(F_i^j)$ for some face $F_i^j \subseteq C_i$, $v_1 = v_E^i(E_i^j)$ for some edge $E_i^j \subseteq C_i$, or $v_1 = v_e^i(E_i^j)$ for some edge $E_i^j \subseteq C_i$. In the first case, the only edges of Γ_{C_i} containing v_1 arise from edges of C_i contained in the face F_i^j, by conditions 2 and 6 from Definition 4.1.2, so v_2 must be equal to $v_E^i(E_i^k)$ for some edge $E_i^k \subseteq F_i^j$. Then by definition of ι, $\iota(v_1) = v_F(\phi_F(F_i^j))$ and $\iota(v_2) = v_E(\phi_E(E_i^k))$. Next, by condition 1 from Lemma 5.1.2, $\phi_E(E_i^k) \subseteq \phi_F(F_i^j)$ since $E_i^k \subseteq F_i^j$. Finally, again by condition 2 of Definition 4.1.2, there is an edge of Γ_C connecting $v_F(\phi_F(F_i^j))$ and $v_E(\phi_E(E_i^k))$ since $\phi_E(E_i^k) \subseteq \phi_F(F_i^j)$. Of course, $\iota(v_1) = v_F(\phi_F(F_i^j))$ and $\iota(v_2) = v_E(\phi_E(E_i^k))$, so $\iota(v_1)$ and $\iota(v_2)$ are connected by an edge. This concludes the first case. The next two cases can be checked similarly, which shows that ι respects edges.

   Now we will see that ι respects weights, which will follow from the way we ordered S and the sequence of edges of C. Let $v_0 \in V(\Gamma_{C_i})$ for some $i \in \{1, 2\}$. Then either there is a face F_i^j of C_i such that $v_0 = v_F^i(F_i^j)$, or there is an edge E_i^k of C_i such that either $v_0 = v_E^i(E_i^k)$ or $v_1^i = v_e(E_i^k)$, by condition 5 from Definition 4.1.2. If $v_0 = v_F^i(F_i^j)$ or $v_0 = v_E^i(E_i^k)$, then the weight of v_0, $W_{S_i}(V_1)$, is 0, by condition 7 from Definition 4.1.2. In this case, by definition of ι, $\iota(v_0) = v_F(\phi_F(F_i^j))$ or $\iota(v_0) = v_E(\phi_E(E_i^k))$. So then $\iota(v_0) \in \operatorname{im}(v_F) \cup \operatorname{im}(v_E)$, so $W_S(\iota(v_0)) = 0$ by condition 7 from Definition 4.1.2. Thus, we see that ι respects weights in this two cases. The remaining case is

$v_0 = v_e^i(E_i^k)$. We will do the case $i = 1$ first, then $i = 2$. For $i = 1$, $v_0 = v_e^1(E_1^k)$ and $\iota(v_0) = v_e(\phi_E(E_1^k))$. So by condition 7 from Definition 4.1.2, $W_{S_1}(v_0) = m_1^k$ and $W_S(v_e(\phi_E E_1^k)) = m^k$. (this last equality follows from the way we ordered the edges of C in the previous paragraph). But $m^k = m_1^k$ for $k \leq k_1^E$, by definition of S, so we see $W_{S_1}(v_0) = W_S(\iota(v_0))$. Next, for $i = 2$, $v_0 = v_e^2(E_2^k)$ and $\iota(v_0) = v_e(\phi_E(E_2^k))$. So by condition 7 from Definition 4.1.2, $W_{S_2}(v_0) = m_2^k$ and $W_S(v_e(\phi_E E_1^k)) = m^{k_1^E+k}$ (this last equality follows from the way we ordered the edges of C in the previous paragraph). But $m^{k_1^E+k} = m_2^k$ for $k_1^E + 1 \leq k \leq k_1^E + k_2^E$, by definition of S, so we see $W_{S_2}(v_0) = W_S(\iota(v_0))$. In both cases, ι respects weights, and it can be seen that S was chosen exactly for this to happen.

2. For any face $F_i^j \subseteq C_i$, let $F^j = \phi_F(F_i^j)$. Then condition 2 holds, since $v_F(F^j) = v_F(\phi_F(F_i^j)) = \iota(v_F^i(F_i^j))$, by definition of ι.

3. By conditions 2 and 4(a) from Lemma 5.1.2, E is the only edge or face of C not in $\text{im}\,(\phi_F) \cup \text{im}\,(\phi_E)$. It can be seen from the definition of ι that this implies $v = v_E(E)$ and $v' = v_e(E)$ are the only vertices not in $\text{im}\,(\iota)$, so condition 3(a) of the lemma holds.

   By condition 4(b) of Lemma 5.1.2, $E \subseteq \phi_F(F_1)$ and $E \subseteq \phi_F(F_2)$. Then by condition 2 from Definition 4.1.2, there is an edge of Γ_C connecting $v_E(E)$ and $v_F(\phi_F(F_1))$. Likewise, there is an edge of Γ_C connecting $v_E(E)$ and $v_F(\phi_F(F_2))$. By definition of ι, $\iota(v_F^1(F_1)) = v_F(\phi_F(F_1))$ and $\iota(v_F^2(F_2)) = v_F(\phi_F(F_2))$. By definition of v, $v = \phi_E(E)$. Combining these last four sentences yields the result that there is an edge of Γ_C connecting v and $\iota(v_F^1(F_1))$, and there is an edge of Γ_C connecting v and $\iota(v_F^2(F_2))$. Next, by condition 4 from Definition 4.1.2, there is an edge of Γ_C connecting $v = v_E(E)$ and $v' = v_e(E)$. This proves condition 3(b) of the lemma. Finally, by condition 7 from Definition 4.1.2, since $v \in \text{im}\,(v_E)$, $W_S(v) = 0$, and since $v' = v_e(E)$, $W_S(v') = z$ (the last equality follows since E was the last edge in the sequence of edges of C, and z was the last integer in the sequence of integers S). This proves condition 3(c).

Q.E.D.

Remarks:

Lemma 5.1.3 gives us a way of combining graphs. Basically, it tells us that, whenever two weighted graph arise from cycle-free cellulations of D^2, we can attach them to a graph with two vertices as depicted in Figure 5.6, and as long as the attaching is done on vertices that correspond to faces, the new weighted graph will also arise from a cycle-free cellulation. Furthermore, the vertices that correspond to faces before the combination still correspond to faces after the combination, which will allow us to repeatedly apply Lemma 5.1.3 to combine the new graph with other graphs.

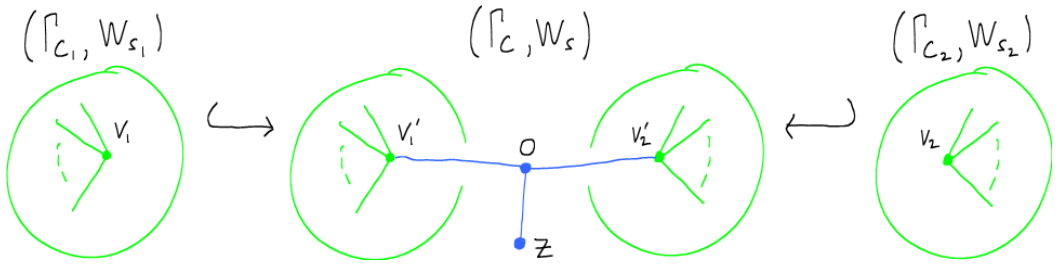

Figure 5.6: The combination of the weighted graphs (Γ_{C_1}, W_{S_1}) and (Γ_{C_2}, W_{S_2}) into a new weighted graph (Γ_C, W_S), where z is an arbitrary integer. The vertex v_1 corresponds to a face of C_1, and the vertex v_2 corresponds to a face of C_2. The images of v_1 and v_2 in the combination, v_1' and v_2', still correspond to faces of C.

Theorem 5.1.4. If M is not homeomorphic to $S^2 \times S^1$, and M is an oriented Seifert fibered space over S^2 with normalized invariants $\{Oo0|b; (\alpha_1, \beta_1), \ldots (\alpha_n, \beta_n)\}$ such that $n \leq 2$ or $b \geq 0$, then M is homeomorphic (not necessarily orientation-preservingly) to $M(\epsilon_C, mult)$ for some cycle-free cellulation C of D^2 and multiplier function $mult$, i.e., M is a cycle-free twisted face-pairing manifold.

Proof. First we will prove the following proposition: Any weighted graph of the form shown in Figure 5.7, with $a_i \geq 0$ for all i, and $a_1 \geq 1$ or $k \geq 2$, arises from a cycle-free cellulation and a sequence of negative integers, with the following convention that if $a_i = 0$ for any i, then the vertex weighted a_i and its adjacent vertex should be deleted. An example of this convention is shown in Figure 5.8. This convention is used to simplify the notation, and over the course of this proof we will point out where discrepancies may arise. We note that, throughout this proof, the decoration from above by an F is not an F-label in the EFe-labeling sense (this would not make sense anyway since there is no EFe-labeling present), but merely an indication that those vertices correspond to a face of the cellulation from which the graph arises.

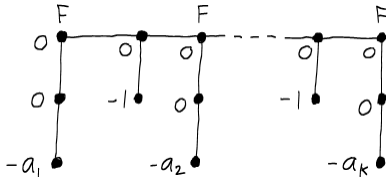

Figure 5.7: A weighted graph arising from a cycle-free cellulation of D^2. Here, $a_i \geq 0$ for all i, and $a_1 \geq 1$ or $k \geq 2$. An 'F' above a vertex indicates that the vertex corresponds to a face of the cellulation.

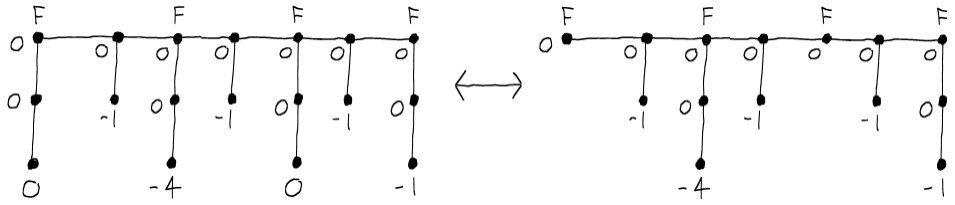

Figure 5.8: Illustration of the convention used when $a_i = 0$ to simplify notation. If we write $a_i = 0$ for some vertex as in the diagram on the left, we really mean the corresponding diagram on the right. Again, an 'F' above a vertex indicates that the vertex corresponds to a face of the cellulation.

Now we will prove the statement. We simply observe the family of cycle-free cellulations and sequence of negative integers in Figure 5.9, and take note of the families of weighted graphs that arise from them.

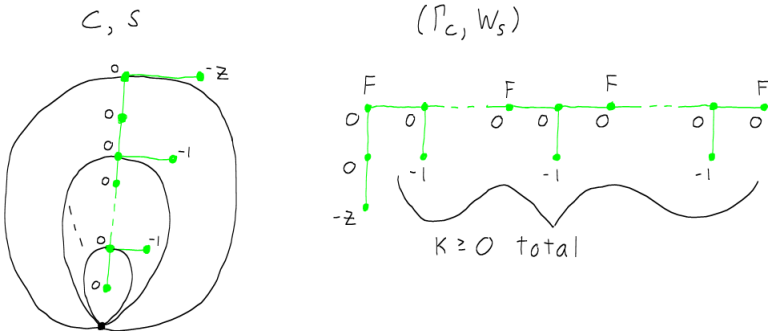

Figure 5.9: Family of cycle-free cellulations C, parametrized by $k \geq 0$, and sequence of negative integers S (which, in this case, is the singleton $\{-z\}$), parametrized by $z \geq 1$, and the corresponding family of induced weighted graph (Γ_C, W_S).

It follows from Lemma 5.1.3 and the remarks following it (see Figure 5.6) that we may combine any two weighted graphs from this family into a new weighted graph as shown in Figure 5.10, and this new weighted graph will also arise from a cycle-free cellulation and sequence of negative integers.

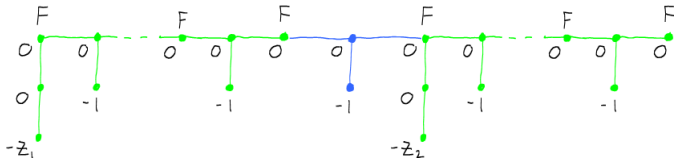

Figure 5.10: Combining two weighted graphs (shown in green) from the family in Figure 5.9 as in Lemma 5.1.3. The resulting weighted graph also arises from a cycle-free cellulation and sequence of negative integers.

It is clear from this that we can obtain all the weighted graphs in Figure 5.7 (assuming the convention as in Figure 5.8) as arising from cycle-free cellulations and sequences of negative integers by iteratively applying this combination process. We note that there must be at least one vertex with negative weight, which is why we ruled out the case $a_1 = 0$, $k = 1$ from Figure 5.7. This proves the proposition, and we are now ready to prove the theorem.

First, we treat the case $n \geq 3$, $b \geq 0$. Within this case, we do the case $b \geq 1$ first. We combine the weighted graphs from Figure 5.7 into a new weighted graph shown in Figure 5.11, and the same requirements hold for this graph: $a_{ij} \geq 1$, $a_{i1} \geq 1$ or $k_i \geq 2$, and also $b \geq 1$, and we use the same convention for $a_{ij} = 0$ as in Figure 5.8. This new weighted graph will arise from a cycle-free cellulation and a sequence of negative integers by Lemma 5.1.3.

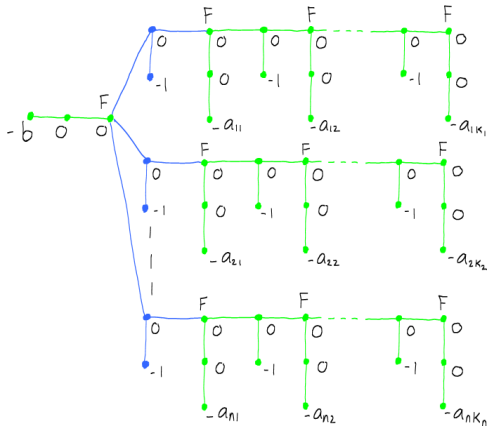

Figure 5.11: Combining weighted graphs (shown in green) from the family in Figure 5.7 as in Lemma 5.1.3. The resulting weighted graph also arises from a cycle-free cellulation and sequence of negative integers.

Now we summarize some facts and put them together to conclude the proof of this case. M is Seifert fibered with normalized invariants as in the statement of the theorem, and with $b \geq 1$, so M is plumbed from the graph in Figure 3.9 by Corollary 3.2.2 (here we can use

Corollary 3.2.2 since $n \geq 3$). The weighted graph in Figure 5.11 ($b \geq 1$ in this graph) arises from a cycle-free cellulation of D^2 and a sequence of negative integers, so by Theorem 4.2.3, the manifold plumbed from this graph is a cycle-free twisted face-pairing manifold. So we have two weighted graphs, shown in Figures 3.9 and 5.11, one whose plumbed manifold is M, and the other whose plumbed manifold is a cycle-free twisted face-pairing manifold. Then by Theorem 3.1.3, M is a cycle-free twisted face-pairing manifold if the graphs can be related to each other by a sequence of moves from Figure 2.2 in Definition 2.0.4. This is precisely what we do in the diagrams shown in Figure 5.12. We note here that, by our convention, if $a_i = 0$ for some i, the vertex weighted a_i and its adjacent vertex should be deleted. This transformation occurs for all vertices weighted a_i during move M2 in Figure 5.12, after which the vertices in the rows have weight a_i in the second graph. Then the second graph shown is in the correct form regardless of the value of a_i.

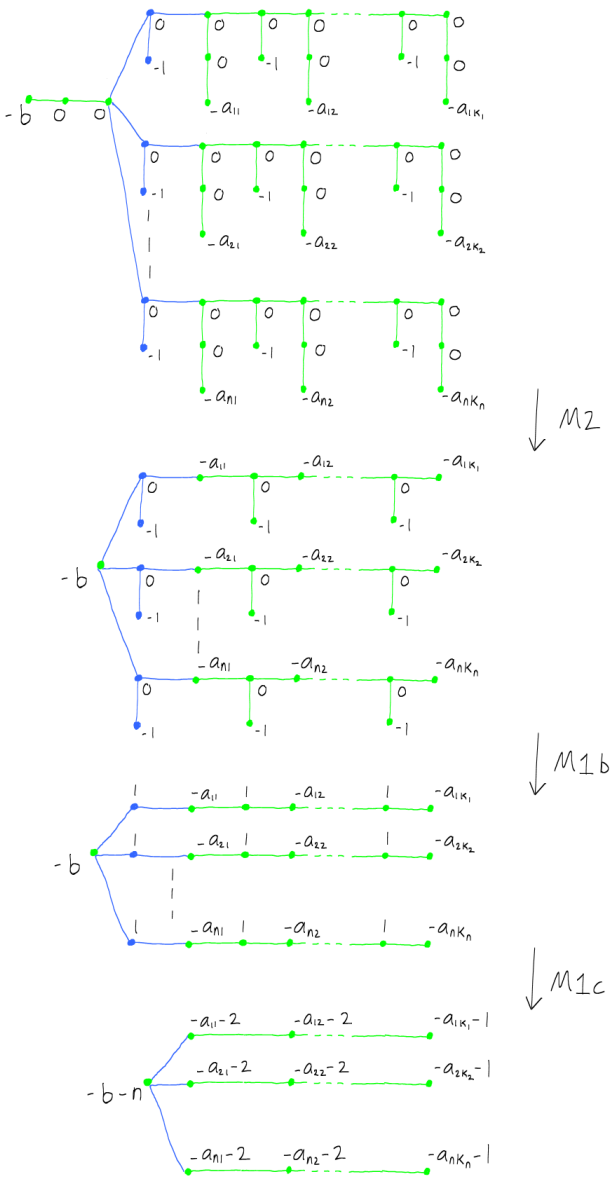

Figure 5.12: Transforming the graph in Figure 5.11 to the graph in Figure 3.9 (with $b \geq 1$) by a sequence of moves from Figure 2.2. This shows M is a cycle-free twisted face-pairing manifold for $n \geq 3$ and $b \geq 1$.

This concludes the proof of the case $n \geq 3$, $b \geq 1$.

Next, we treat the case $n \geq 3$, $b = 0$. We combine the weighted graphs from Figure 5.7 into a new weighted graph shown in Figure 5.13, with the same requirements and conventions holding as in the proof of the case $b \geq 1$.

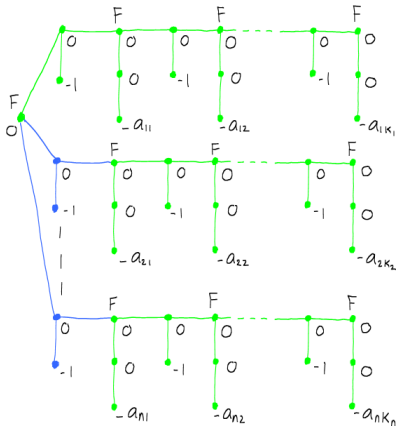

Figure 5.13: Combining weighted graphs (shown in green) from the family in Figure 5.7 as in Lemma 5.1.3. The resulting weighted graph also arises from a cycle-free cellulation and sequence of negative integers.

For all the same reasons as in the proof of the case $b \geq 1$ in the previous paragraph, the transformation between diagrams shown in Figure 5.14 proves that M is a cycle-free twisted face-pairing manifold.

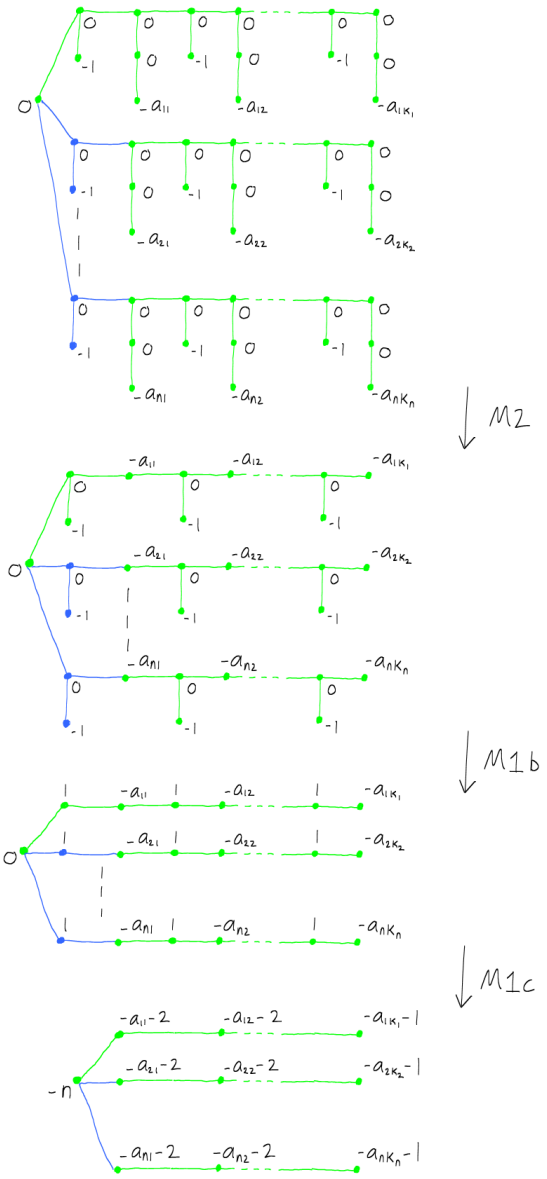

Figure 5.14: Transforming the graph in Figure 5.13 to the graph in Figure 3.9 (with $b = 0$) by a sequence of moves from Figure 2.2. This shows M is a cycle-free twisted face-pairing manifold for $n \geq 3$ and $b = 0$.

This proves the case $n \geq 3$, $b = 0$, and thus proves the case $n \geq 3$.

Finally, we treat the case $n \leq 2$. We will be using facts about lens spaces here, and the reader may consult Orlik [9] for these, especially page 99. Since $n \leq 2$, M is a lens space, and M is not homeomorphic to $S^2 \times S^1$ by assumption. Now, all lens spaces other than

$S^2 \times S^1$ are homeomorphic to a lens space $L(p,q)$ with $\frac{p}{q} < 0$ (by reversing orientation if $\frac{p}{q} > 0$). Any number $\frac{p}{q} < 0$ is equal to a continued fraction $[-z_1 - 1, -z_2 - 2, \cdots - z_k - 2]$ with each $z_i \geq 0$ (see Figure 3.8 for an explanation of this notation). This implies that M is homeomorphic to the manifold plumbed from a graph of the form in Figure 5.15.

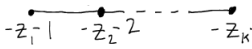

Figure 5.15: Plumbing graph for the lens space $L(p,q)$, to which M is homeomorphic, where $\frac{p}{q} = [-z_1 - 1, -z_2 - 2, \cdots - z_k - 2]$.

Now we summarize some facts and put them together to conclude the proof of this case. M is homeomorphic to $L(p,q)$ which is homeomorphic to the manifold plumbed from the weighted graph of Figure 5.15. The weighted graph in Figure 5.7 arises from a cycle-free cellulation of D^2 and a sequence of negative integers, so by Theorem 4.2.3, the manifold plumbed from this graph is a cycle-free twisted face-pairing manifold. So we have two weighted graphs, shown in Figures 5.7 and 5.15, one whose plumbed manifold is M, and the other whose plumbed manifold is a cycle-free twisted face-pairing manifold. Then by Theorem 3.1.3, M is a cycle-free twisted face-pairing manifold if the graphs can be related to each other by a sequence of moves from Figure 2.2 in Definition 2.0.4. This is precisely what we do in the diagrams shown in Figure 5.16. We note here that, by our convention, if $a_i = 0$ for some i, the vertex weighted a_i and its adjacent vertex should be deleted. This transformation occurs for all vertices weighted a_i during move M2 in Figure 5.16, after which the vertices on the top row have weight a_i in the second graph. Then the second graph shown is in the correct form regardless of the value of a_i.

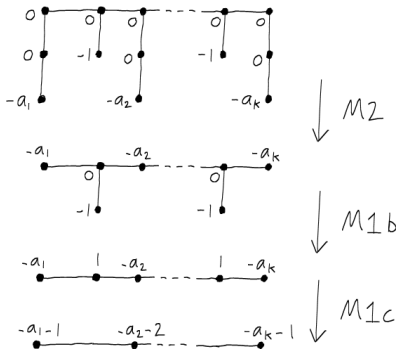

Figure 5.16: Transforming the graph in Figure 5.7 to the graph in Figure 5.15 by a sequence of moves from Figure 2.2. This shows M is a cycle-free twisted face-pairing manifold for $n \leq 2$.

This concludes the proof of the case $n \leq 2$, and thus the proof of the theorem. Q.E.D.

Theorem 5.1.5. If M is not homeomorphic to $S^2 \times S^1$, and M is an oriented Seifert fibered space over S^2 with normalized invariants $\{Oo0\big|b; (\alpha_1, \beta_1), \ldots (\alpha_n, \beta_n)\}$, then M is homeomorphic (not necessarily orientation-preservingly) to $M(\epsilon_C, mult)$ for some cycle-free cellulation C of D^2 and multiplier function $mult$ (i.e., M is a cycle-free twisted face-pairing manifold) if and only if $n \leq 2$, $b \geq 0$, or $b \leq -n$.

Proof. For one implication, Let M be an oriented Seifert fibered space as above with $n \leq 2$, $b \geq 0$, or $b \leq -n$. If $n \leq 2$ or $b \geq 0$, then the conclusion follows exactly from Theorem 5.1.4. Then assume $b \leq -n$. By reversing the orientation of M, we obtain an oriented Seifert fibered space M' with normalized invariants $\{Oo0\big|c; (\alpha_1, \alpha_1 - \beta_1), \ldots (\alpha_n, \alpha_n - \beta_n)\}$, where $c = -b - n$. This follows from Section 4.4 of [6]. Since $b \leq -n$, $c \geq 0$, so Theorem 5.1.4 applies to M', which is just M with the orientation reversed. So in this case M is also a cycle-free twisted face-pairing manifold.

For the other implication, let M be an oriented Seifert fibered space as above with $n \geq 3$ and $-n < b < 0$. By reversing the orientation of M, we obtain an oriented Seifert fibered space M' with normalized invariants $\{Oo, 0\big|c; (\alpha_1, \alpha_1 - \beta_1), \ldots (\alpha_n, \alpha_n - \beta_n)\}$, where $c = -b - n$. Since $-n < b < 0$, $-n < c < 0$. So by Theorem 5.1.1, neither M nor M' is orientation-preservingly homeomorphic to a cycle-free twisted face-pairing manifold. Since M' is just M with the orientation reversed, this implies M is not (orientation-preservingly or -reversingly) homeomorphic to a cycle-free twisted face-pairing manifold. Q.E.D.

5.2 Spherical Space Forms

In Chapter 1, we defined Seifert fibered spaces in terms of a set of invariants. We also defined spherical space forms and gave a description of them as Seifert fibered spaces of S^2 with a specific set of invariants. When the invariants where chosen to be normalized and so that $b \geq -1$, they uniquely determined the spherical manifold up to homeomorphism, except for the lens spaces. Also, these manifolds fit nicely into different families according to their fundamental groups, or equivalently, according to their Seifert invariants. This grouping is summarized in Table 5.1.

Table 5.1: The five families of spherical space forms and their corresponding normalized Seifert invariants.

Family of Spherical Manifolds	Normalized Seifert Invariants with $b \geq -1$
Lens Spaces	$\{Oo0 \vert b; (\alpha_1, \beta_1), \ldots (\alpha_n, \beta_n)\}$ $0 \leq n \leq 2$
Prism Manifolds	$\{Oo0 \vert b; (2,1), (2,1), (\alpha_3, \beta_3)\}$
Tetrahedral	$\{Oo0 \vert b; (2,1), (3, \beta_2), (3, \beta_3)\}$
Octahedral	$\{Oo0 \vert b; (2,1), (3, \beta_2), (4, \beta_3)\}$
Icosahedral	$\{Oo0 \vert b; (2,1), (3, \beta_2), (5, \beta_3)\}$

We now draw conclusions using Theorem 5.1.5 and Table 5.1.

All the lens spaces are cycle-free twisted-face-pairing manifolds.

There is an infinite family of prism manifolds having invariants $\{Oo0\vert -1; (2,1), (2,1), (\alpha_3, \beta_3)\}$ $(0 < \beta_3 < \alpha_3,\ (\alpha_3, \beta_3) = 1)$ that are not cycle-free twisted face-pairing manifolds, while the rest of the prism manifolds are.

There are only 3 manifolds from the tetrahedral family that are not cycle-free twisted face-pairing manifolds, namely the three with invariants:

1. $\{Oo0\vert -1; (2,1), (3,1), (3,1)\}$
2. $\{Oo0\vert -1; (2,1), (3,1), (3,2)\}$
3. $\{Oo0\vert -1; (2,1), (3,2), (3,2)\}$

There are only 4 manifolds from the octahedral family that are not cycle-free twisted face-pairing manifolds, namely the four with invariants:

1. $\{Oo0\vert -1; (2,1), (3,1), (4,1)\}$
2. $\{Oo0\vert -1; (2,1), (3,1), (4,3)\}$
3. $\{Oo0\vert -1; (2,1), (3,2), (4,1)\}$
4. $\{Oo0\vert -1; (2,1), (3,2), (4,3)\}$

There are only 8 manifolds from the icosahedral family that are not cycle-free twisted face-pairing manifolds, namely the eight with invariants:

1. $\{Oo0\Big| -1; (2,1), (3,1), (5,1)\}$
2. $\{Oo0\Big| -1; (2,1), (3,1), (5,2)\}$
3. $\{Oo0\Big| -1; (2,1), (3,1), (5,3)\}$
4. $\{Oo0\Big| -1; (2,1), (3,1), (5,4)\}$
5. $\{Oo0\Big| -1; (2,1), (3,2), (5,1)\}$
6. $\{Oo0\Big| -1; (2,1), (3,2), (5,2)\}$
7. $\{Oo0\Big| -1; (2,1), (3,2), (5,3)\}$
8. $\{Oo0\Big| -1; (2,1), (3,2), (5,4)\}$

The first manifold on this list is the Poincarè homology 3-sphere, so it is not a cycle-free twisted face-pairing manifold.

Bibliography

[1] J. W. Cannon, W. J. Floyd, and W. R. Parry, *Introduction to Twisted Face-Pairings*, Mathematical Research Letters 7 (2000), 477-491.

[2] J. W. Cannon, W. J. Floyd, and W. R. Parry, *Twisted Face-Pairing 3-Manifolds*, Transactions of the American Mathematical Society 354 (2002), 2369-2397.

[3] J.W. Cannon, W.J. Floyd, and W.R. Parry, *Heegaard Diagrams and Surgery Descriptions for Twisted Face-Pairing 3-Manifolds*, Algebr. Geom. Topol. 3 (2003) 235285 (electronic).

[4] J.W. Cannon, W.J. Floyd, and W.R. Parry, *A Survey of Twisted Face-Pairing 3-Manifolds*, preprint.

[5] Nathan Dunfield, William Thurston, *Finite Covers of Random 3-Manifolds*, Inventiones Mathematicae 166 (2006) 457-521.

[6] J.M. Montesinos, *Classical Tesselations and Three-Manifolds*, Springer-Verlag, New York, 1987.

[7] Walter Neumann, *An Invariant of Plumbed Homology Spheres*, Lecture Notes in Mathematics Volume 788, 1980, pp 125-144.

[8] Walter Neumann, *A Calculus for Plumbing Applied to the Topology of Complex Surface Singularities and Degenerating Complex Curves*, Transactions of the American Mathematical Society Volume 268, Number 2, December 1981

[9] Peter Orlik, *Seifert Manifolds*, Springer-Verlag, New York, 1972.

[10] Nikolai Saveliev, R.V. Gamkrelidze, A. Vassiiev, *Invariants of Homology 3-Spheres*, Berlin: Springer Berlin, 2010.

[11] Peter Scott, *The Geometries of 3-Manifolds*, Bull. London Math. Soc. 15 (1983), 401-487.

[12] Friedhelm Waldhausen, *Eine Klasse von 3-dimensionalen Mannigfaltigkeiten. I*, 1967, Inventiones Mathematicae Volume 3, Number 4, 308-333.